

**ANALYSIS OF RADIONUCLIDE DEPOSITION RATIOS FROM THE
FUKUSHIMA-DAIICHI INCIDENT**

A Thesis

by

MICHEAL RASHAUN SMITH

Submitted to the Office of Graduate and Professional Studies of
Texas A&M University
in partial fulfillment of the requirements for the degree of

MASTER OF SCIENCE

Chair of Committee,	Craig Marianno
Committee Members,	John W. Poston, Sr.
	Sunil P. Khatri
Head of Department,	Yassin A. Hassan

August 2014

Major Subject: Health Physics

Copyright 2014 Micheal Rashaun Smith

ABSTRACT

Consequence management radiological dose assessors make several assumptions in dose projections regarding radionuclide depositions following a radiological release from a nuclear power plant. During training and exercises these coordinators and dose assessors make assumptions that the radionuclide deposition ratios will remain constant, only varying in terms of radioactive decay and weathering. This assumption is sometimes made regardless of large spatial and terrain variations. Following the Fukushima-Daiichi accident, the National Nuclear Security Administration's Consequence Management Response Teams (CMRT) assisted in consequence management operations in Japan. Part of their work included taking air samples and *in situ* measurements using high purity germanium detectors throughout certain areas of the country. On this research the validity of the aforementioned assumption was examined by analysis of the *in situ* measurements obtained by the U.S. response teams and the Japan Atomic Energy Agency (JAEA). Using isotopic ratios for a LWR core-damage accident, from FRMAC Manual Volume 3, a comparison was made with the collected *in situ* measurement data to determine how the FRMAC values compared against actual measured data. The main radionuclides considered in this evaluation were ^{134}Cs , ^{136}Cs , ^{137}Cs and ^{131}I . The goal of this comparison was to determine the validity of the training and exercise assumptions with regard to a real incident.

TABLE OF CONTENTS

	Page
ABSTRACT	ii
TABLE OF CONTENTS	iii
LIST OF FIGURES.....	v
LIST OF TABLES	vii
INTRODUCTION.....	1
Objective.....	1
Two Major Radiological Incidents (Chernobyl and Fukushima)	2
Chernobyl Accident	4
Fukushima-Daiichi Incident.....	10
Federal Radiological Monitoring and Assessment Center (FRMAC)	
Radiological Assessment Assumptions	18
Previous Research/Analysis.....	23
METHODS AND MATERIALS	33
DOE/NNSA CMRT Data	33
JAEA ¹³⁴ Cs and ¹³⁷ Cs Variation Data.....	37
RESULTS.....	39
DOE/NNSA CMRT Data	39
Comparing FRAMC Assessment Manual Vol. 3 Values to DOE/NNSA	
Fukushima <i>in situ</i> Measurements.....	46
JAEA ¹³⁴ Cs and ¹³⁷ Cs Variation Data.....	47
DISCUSSION	51
CONCLUSIONS.....	56
REFERENCES.....	59

LIST OF FIGURES

	Page
Fig. 1. RMBK-1000 reactor design.....	5
Fig. 2. Deposition of ^{137}Cs in Belarus as a result of the Chernobyl Accident.....	8
Fig. 3. Deposition of ^{137}Cs in Ukraine as a result of the Chernobyl Accident.....	9
Fig. 4. Location of epicenter of the earthquake is shown with the resulting seismic intensity throughout Japan.	12
Fig. 5. Tsunami waves approaching the Fukushima Daiichi nuclear power plant, in a photo released by TEPCO	13
Fig. 6. Fukushima-Daiichi release plume from aerial measurements taken by U.S. and Japan teams.....	17
Fig. 7. Major steps in a radiological assessment [adapted from NCRP (1984a)].	22
Fig. 8. $^{134}\text{Cs}/^{137}\text{Cs}$ isotopic activity ratio for US IMS stations (1 σ error bars)	25
Fig. 9. $^{136}\text{Cs}/^{137}\text{Cs}$ isotopic activity ratio for US IMS stations (1 σ error bars)	26
Fig. 10. Contour maps of depositions for several radionuclides; and activity ratios for $^{129\text{m}}\text{Te}/^{137}\text{Cs}$, $^{131}\text{I}/^{137}\text{Cs}$, and $^{129\text{m}}\text{Te}/^{131}\text{I}$ through Japan are shown. Activities from March 29 th , 2011 are shown.	28
Fig. 11. Amount of rainfall in Japan on March 15-16 th and March 21, based on AMeDAS	29
Fig. 12. $^{134}\text{Cs}/^{137}\text{Cs}$ activity ratios for 158 <i>in situ</i> measurements. Figure courtesy of Lawrence Livermore National Laboratory.....	30
Fig. 13. $^{134}\text{Cs}/^{137}\text{Cs}$ activity ratios for 174 air samples. Figure courtesy of Lawrence Livermore National Laboratory.	31
Fig. 14. $^{134}\text{Cs}/^{137}\text{Cs}$ net counts ratio with respect to the date the measurements were taken.	40
Fig. 15. Map displaying <i>in situ</i> measurement locations with highlighted locations for the $^{134}\text{Cs}/^{137}\text{Cs}$ values with uncertainties greater than 20%.	41

Fig. 16. $^{136}\text{Cs}/^{137}\text{Cs}$ net counts ratio with respect to the date the measurements were taken.	43
Fig. 17. $^{131}\text{I}/^{137}\text{Cs}$ net counts ratio with respect to the date the measurements were taken.	44
Fig. 18. Map displaying <i>in situ</i> measurement locations with highlighted locations for highest $^{131}\text{I}/^{137}\text{Cs}$ values.	45
Fig. 19. Location of the 1016 <i>in situ</i> measurements for the 2nd measurement.....	49
Fig. 20. Map of Japan with <i>in situ</i> measurement locations and DEMs.....	54
Fig. A- 1. 2nd Measurement <i>in situ</i> measurement locations.	62
Fig. A- 2. 3rd Prophase <i>in situ</i> measurement locations.....	63
Fig. A- 3. 3rd Anaphase <i>in situ</i> measurement locations.....	64
Fig. A- 4. 4th measurement <i>in situ</i> measurement locations	65
Fig. A- 5. Plot for $^{134}\text{Cs}/^{137}\text{Cs}$ concentration ratios from 2nd measurement.....	66
Fig. A- 6. Plot for $^{134}\text{Cs}/^{137}\text{Cs}$ concentration ratios from 3rd prophase measurement	66
Fig. A- 7. Plot for $^{134}\text{Cs}/^{137}\text{Cs}$ concentration ratios from 3rd anaphase measurement.	67
Fig. A- 8. Plot for $^{134}\text{Cs}/^{137}\text{Cs}$ concentration ratios from 4th measurement.....	67

LIST OF TABLES

	Page
Table 1. Estimated reactor core inventory and estimated radionuclide releases from the Chernobyl accident.....	6
Table 2. Six Units of the Fukushima-Daiichi NPS	10
Table 3. Iodine/ ¹³⁷ Cs ratio and its associated standard deviation are given for data from CMRT and DOD data.....	32
Table 4. Radionuclide concentrations relative to ¹³⁷ Cs for a LWR core-damage accident are given for specific times after reactor shutdown	35
Table 5. Average ratios and standard deviations for the deposition ratios of interest (¹³⁴ Cs/ ¹³⁷ Cs, ¹³⁶ Cs/ ¹³⁷ Cs, ¹³¹ I/ ¹³⁷ Cs) with respect to different times after shutdown.	46
Table 6. The highest ¹³¹ I/ ¹³⁷ Cs values located to the southwest of the nuclear power plants are given along with their associated uncertainty, latitude and longitude	47
Table 7. Average and decay corrected average of ¹³⁴ Cs/ ¹³⁷ Cs concentration ratio from JAEA data.....	50

INTRODUCTION

Objective

Today one of the major debates around the world is the fate and danger of nuclear energy. Harnessing nuclear energy for electricity production came after the development of the first nuclear bomb, which was first tested in 1945. The testing of nuclear weapons and the display of their power has instilled fear in many people, which has led to protests against nuclear power all over the world. Accidents at nuclear power plants over the years have added to this fear. There have been small-scale accidents, but the major well-known accidents, are the Three Mile Island, Chernobyl and Fukushima-Daiichi incidents. These three incidents have greatly influenced how the public perceives nuclear risk. With everything some risk is involved, regardless of how small that risk, people and countries need to be prepared to adapt and handle any problems that may occur.

All over the world there are emergency response professionals that are trained to respond effectively and provide support for several different emergency scenarios. A nuclear or radiological emergency is no different. There are several teams trained to specifically respond to emergencies of this sort. Radiological emergencies do not occur often but it is always necessary for emergency responders to be prepared if an emergency ever were to occur. Radiological emergency response professionals engage in many training exercises to ensure that they are always prepared to respond to an emergency. For these exercises the response scenarios can only be simulated and to do this the professionals make assumptions for the scenario at hand. These assumptions

help to create ideal situations for the responders, which may not always be the case during an actual nuclear/radiological incident.

The assumptions that are made are practical but, to ensure that the response professionals are prepared for any situation, it is necessary to have assumptions that can and will relate as closely as possible to a real scenario. During exercises for radiological emergencies one main assumption typically made is that radionuclide deposition ratios will remain constant, only varying in terms of decay and weathering. Assumptions like these help to simplify the exercise scenarios and create an ideal response situation. The recent Fukushima incident was not an ideal situation since there were many releases along with drastic changes to the weather conditions. With the Fukushima incident not being an ideal situation, provides the perfect opportunity to determine if the aforementioned assumption will hold true outside of exercises. This research helped to validate whether or not radionuclide deposition ratios will remain constant, when there are large spatial and terrain variations along with inclement weather.

Two Major Radiological Incidents (Chernobyl and Fukushima)

The two most recent nuclear reactor accidents that resonate in many people's minds are the Chernobyl and Fukushima incidents. From Chernobyl to the more recent Fukushima incident a great deal of progress has been made regarding the response to radiological incidents and the capabilities of the responders. With better capabilities the response to the Fukushima event and the data available should be superior to that of the Chernobyl accident. There are very large sets of data for both events but with the Fukushima event being more recent, it is pertinent to analyze the data from the event.

Radiological responses may never involve an ideal situation like many exercises in which emergency response professionals participate. The Chernobyl and Fukushima incidents show how far from ideal real world scenarios can be. The International Nuclear and Radiological Event Scale (INES) was introduced in 1990 by the International Atomic Energy Agency (IAEA). The INES categorizes events on a scale of 1-7, where 7 is a major accident. According to the INES scale there have only been two major accidents, those at Chernobyl and Fukushima. Chernobyl was considered a level 7 because of the magnitude of the radiological release, but Fukushima was initially considered a 4 on the INES scale. After much political pressure the Fukushima incident was categorized as a level 7. When comparing the releases of the Chernobyl and Fukushima incidents the Japanese authorities estimated that the radioactivity released from the Fukushima plant was only about 10% of that was released from the Chernobyl plant (Nuclear Energy Institute, 2011). The Nuclear and Industrial Safety Agency estimated that the total discharge from the Fukushima-Daiichi plant was approximately 1.6×10^{17} Bq for ^{131}I and 1.5×10^{16} Bq for ^{137}Cs (Nuclear Emergency Response Headquarters GOJ, 2011). The estimated total discharge from the Chernobyl accident was 1.76×10^{18} Bq for ^{131}I and 8.5×10^{16} Bq for ^{137}Cs (Nuclear Energy Agency, 2002). There are clear differences in the magnitude of the releases but this was most likely due to factors such as reactor design and containment, along with completely different accident scenarios.

Chernobyl Accident

In 1986, the Chernobyl accident took place and sparked a change in how the public perceived the risk of nuclear power. The Chernobyl nuclear power plant was located in Ukraine about 20 km south of the border of Belarus. On August 25th, 1986 Unit 4 of the power plant was scheduled to be shut down for routine maintenance. The Unit 4 reactor was a RBMK-1000 Soviet-designed reactor that was a graphite moderated boiling light water reactor. A basic design of the RBMK-1000 is shown in Fig. 1 (NEA OECD, 2002). The reactor fuel was uranium dioxide enriched to 2% ²³⁵U. The RBMK-1000 design provided a direct steam feed from the reactor to the turbines. The water in the reactor fuel channels acted as a coolant and also provided steam to power the turbines. While the routine shut down took place, personnel decided to test if the slowing turbines could provide enough power to operate the emergency equipment and cooling systems, until the emergency power supply could take over. During the turbine test there were inadequate safety precautions and the personnel implementing the test were not aware of the nuclear safety implications, because they did not have adequate knowledge in the areas and did not speak with the appropriate personnel prior to the test. The turbine test had been performed during a shutdown before but the results were inconclusive, which led to personnel repeating the experiment.

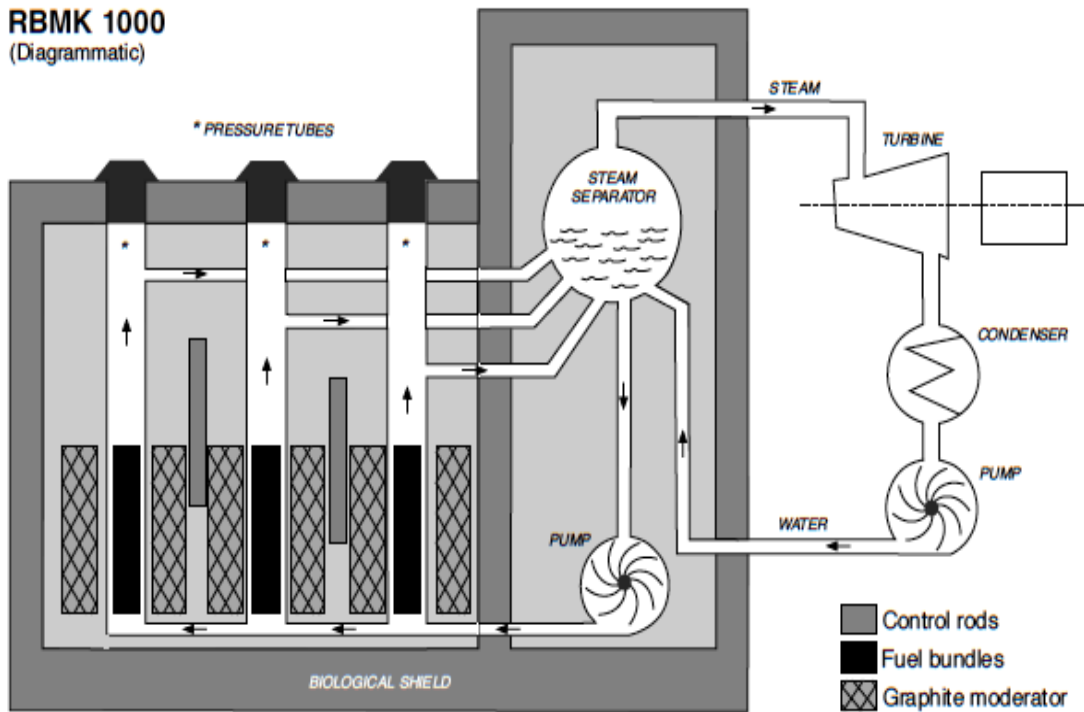


Fig. 1. RBMK-1000 reactor design (NEA OECD, 2002).

The test ultimately resulted in two explosions that led to fuel, core components and structural items along with other hot and highly radioactive debris being released into the air and environment. The explosions led to a wide spread release of fission products and noble gases to the northwest of the plant. Graphite fires started in the Unit 4 building giving rise to clouds of steam and dust, which contributed to the dispersion of radionuclides and fission products high into the atmosphere. The radiological release from the accident continued for about 20 days. Estimates of radionuclide releases during the Chernobyl accident are given in Table 1. (NEA OECD, 2002).

Table 1. Estimated reactor core inventory and estimated radionuclide releases from the Chernobyl accident (NEA OECD, 2002).

Reactor Core Inventory (April 26 th , 1986)			Total release during the accident	
Nuclide	Half-life	Activity (PBq)	% of inventory released	Activity (PBq)
¹³³ Xe	5.3 d	6500	100	6500
¹³¹ I	8.0 d	3200	50-60	~1760
¹³⁴ Cs	2.0 y	180	20-40	~54
¹³⁷ Cs	30.0 y	280	20-40	~84
¹³² Te	78.0 h	2700	25-60	~1150
⁸⁹ Sr	52.0 d	2300	4-6	~115
⁹⁰ Sr	28.0 y	200	4-6	~10
¹⁴⁰ Ba	12.8 d	4800	4-6	~240
⁹⁵ Zr	65.0 f	5600	3.5	196
⁹⁹ Mo	67.0 h	4800	>3.5	>168
¹⁰³ Ru	39.6 d	4800	>3.5	>168
¹⁰⁶ Ru	1.0 y	2100	>3.5	>73
¹⁴¹ Ce	33.0 d	5600	3.5	196
¹⁴⁴ Ce	285.0 d	3300	3.5	~116
²³⁹ Np	2.4 d	27000	3.5	~95
²³⁸ Pu	86.0 y	1	3.5	0.035
²³⁹ Pu	24400.0 y	0.85	3.5	0.03
²⁴⁰ Pu	6580.0 y	1.2	3.5	0.042
²⁴¹ Pu	13.2 y	170	3.5	~6
²⁴² Cm	163.0 d	26	3.5	~0.9

The source term for the accident was extremely complex due to the graphite fires, which created extensive releases of fuel material and attributed to a long radiological release. During the first days of the release, weather conditions were changing constantly causing variations in the direction and dispersion of the release from the accident.

Radionuclide depositions depend greatly on the weather conditions, especially wind and rainfall. Particle size also factored into the final deposition of the radionuclides. Larger

particles tended to deposit closer to the plant than small particles. The largest particles released from the Chernobyl accident were primarily fuel particles. The largest particles deposited within 100 km of the reactor. Smaller particles traveled large distances within the plume until finally depositing, mostly due to rainfall (NEA OECD, 2002).

Contamination from the Chernobyl reactor was found on the ground in almost every country in the northern hemisphere. Deposition of ^{137}Cs in Belarus and Ukraine as a result of the Chernobyl accident is shown in Fig. 3 and 4, respectively. For the Chernobyl accident ^{137}Cs was used to characterize the magnitude of the radionuclide depositions on the ground. I-131 was not used for this characterization because its half-life is extremely short compared to ^{137}Cs . Early maps created in the former Soviet Union were based on the small number of ^{131}I measurements; even though ^{137}Cs was used as a guide to characterize the magnitude of the ground depositions. From the early maps it was found that the deposition densities of ^{131}I to ^{137}Cs varied spatially throughout Belarus. The ratios varied from about 5 to 10 (NEA OECD, 2002). The ^{131}I to ^{137}Cs ratio was not studied much in other countries after the Chernobyl incident though. The variance in the ^{131}I to ^{137}Cs ratio was most likely due to the constantly changing weather conditions at the time of the accident. In regards to radionuclide depositions little information was found pertaining to the Chernobyl incident.

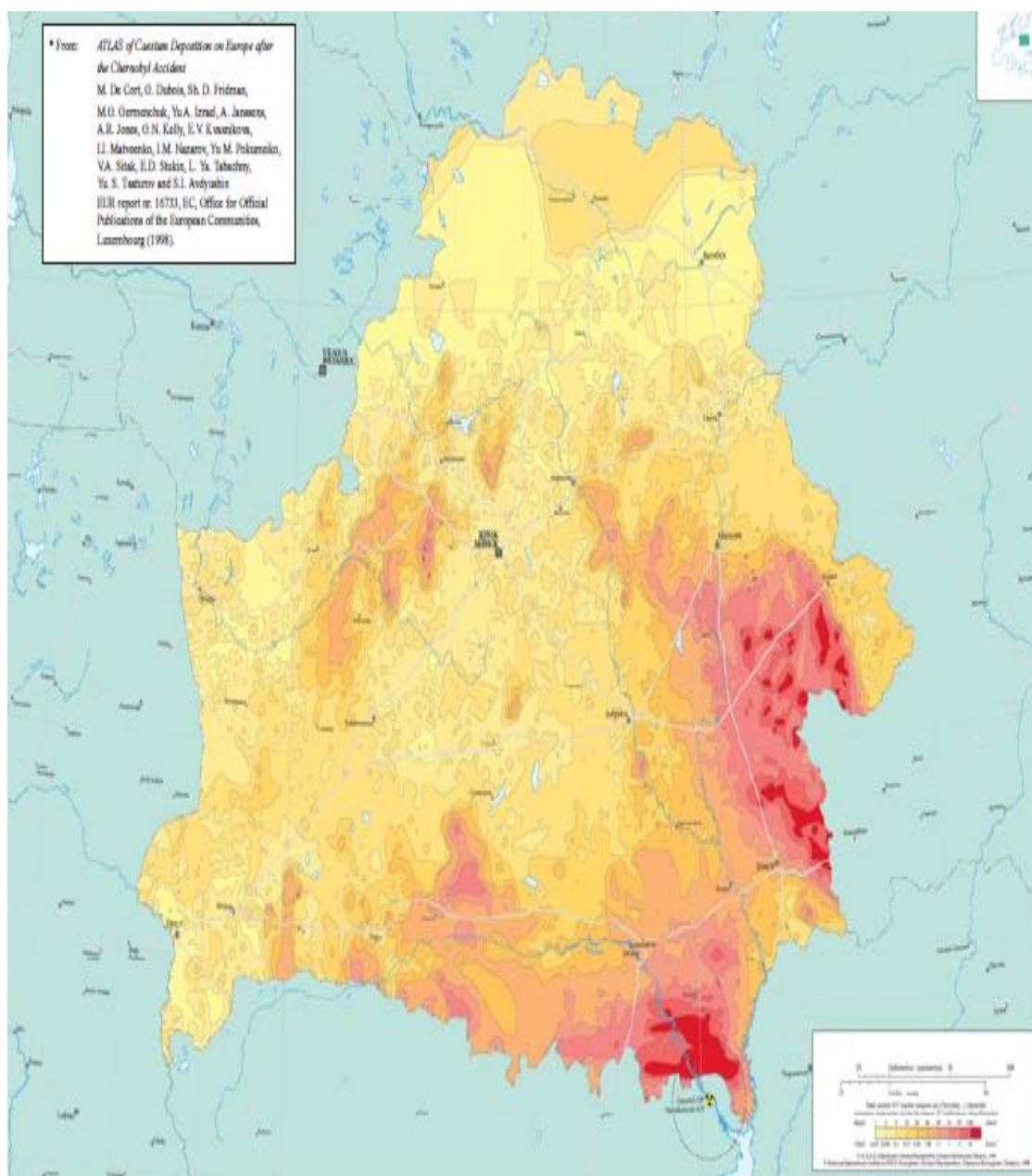


Fig. 2. Deposition of ^{137}Cs in Belarus as a result of the Chernobyl Accident. (NEA OECD, 2002).

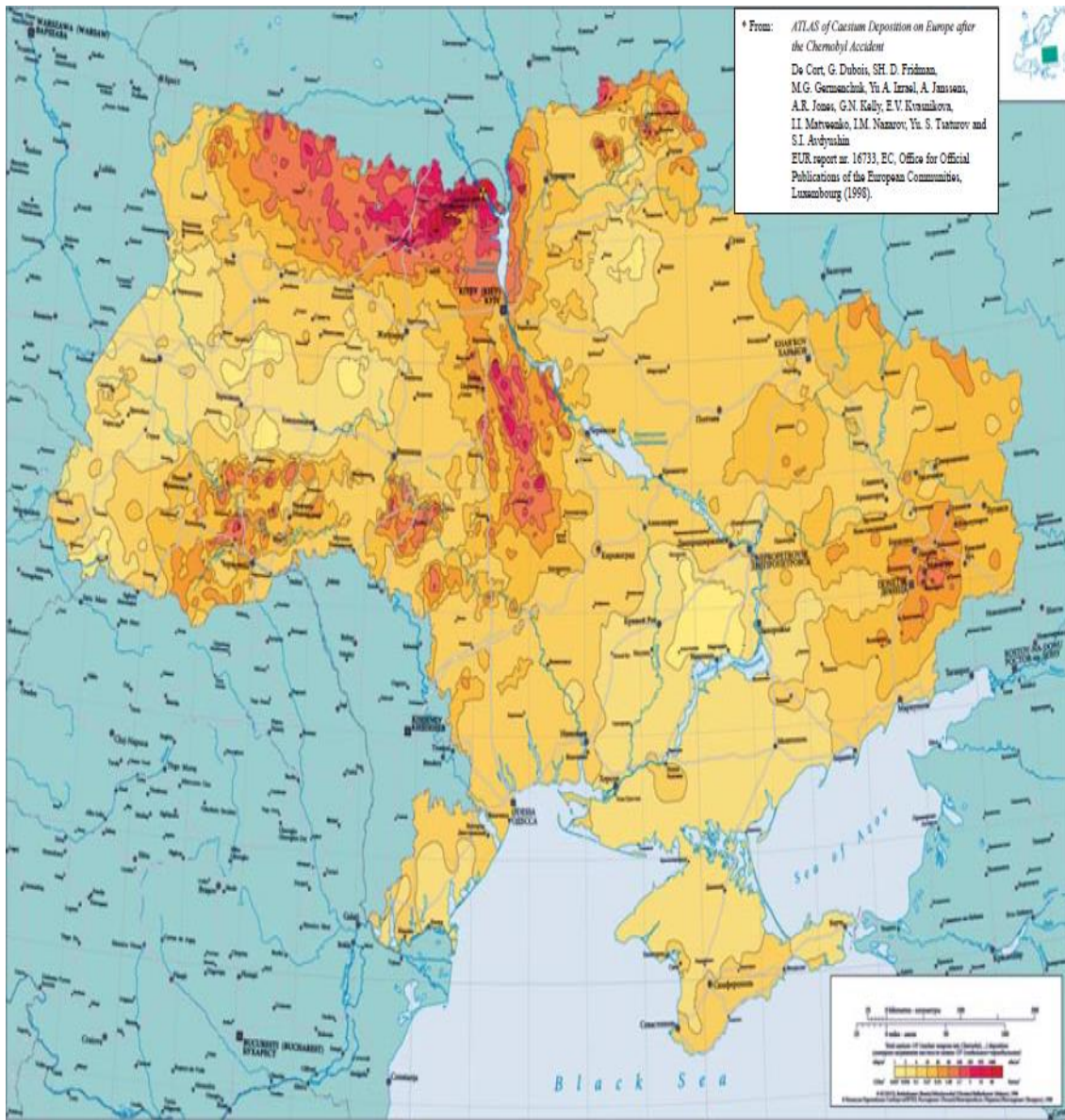


Fig. 3. Deposition of ^{137}Cs in Ukraine as a result of the Chernobyl Accident. (NEA OECD, 2002).

Fukushima-Daiichi Incident

Fukushima Daiichi Nuclear Power Station (NPS) was located in the Fukushima Prefecture, facing the Pacific Ocean. The area of the site was approximately 864.9 acres and the station was operated by the Tokyo Electric Power Company (TEPCO).

Fukushima-Daiichi was the first NPS to be operated by TEPCO; the first unit was commissioned in March 1971. The NPS had a total of six reactors with a total electric generating capacity of about 4.696 million kilowatts. Information for all six of the Fukushima-Daiichi units is shown in Table 2.

Table 2. Six Units of the Fukushima-Daiichi NPS.

	Unit 1	Unit 2	Unit 3	Unit 4	Unit 5	Unit 6
Electric output (MW)	460	784	784	784	784	1100
Start of construction	Sep. 1967	May 1969	Oct. 1970	Sep. 1972	Dec. 1971	May 1973
Commissioning	Mar. 1971	Jul. 1974	Mar. 1976	Oct. 1978	Apr. 1978	Oct. 1979
Decommissioning	Apr. 2012	Apr. 2012	Apr. 2012	Apr. 2012		
Reactor type	BWR-3	BWR-4	BWR-4	BWR-4	BWR-4	BWR-5
Containment type	Mark I	Mark I	Mark I	Mark I	Mark I	Mark II
Number of fuel assemblies	400	548	548	548	548	764
Number of control rods	97	137	137	137	137	185

According to the Government of Japan (GOJ) report to the IAEA, the chronological events of the incident were the following. On March 11th, 2011 an earthquake occurred

in the Pacific Ocean off the coast of Japan registering a magnitude of 9.0 on the Richter scale. Several aftershocks, all which had a magnitude of 5 or greater, followed the earthquake. The location of the epicenter of the earthquake with respect to the location of several nuclear power plants in Japan can be seen in Fig. 5 (Nuclear Emergency Response Headquarters GOJ, 2011). The magnitude 9.0 earthquake caused a massive tsunami, which arrived at the Aomori, Iwate, Miyagi, and Fukushima Prefectures twenty-eight minutes after the initial earthquake. The damage from the earthquake and tsunami resulted in a flooded area of about 561 km², along with damage to approximately 475,000 structures and approximately 4,000 spots of road damage, 7280 spots of damage to railways and 4 million households were left without electricity (Nuclear Emergency Response Headquarters GOJ, 2011). Following the damage from the tsunami a nuclear accident occurred at the Fukushima-Daiichi NPS. The damage from the tsunami contributed to a lengthy radiological release throughout Japan.

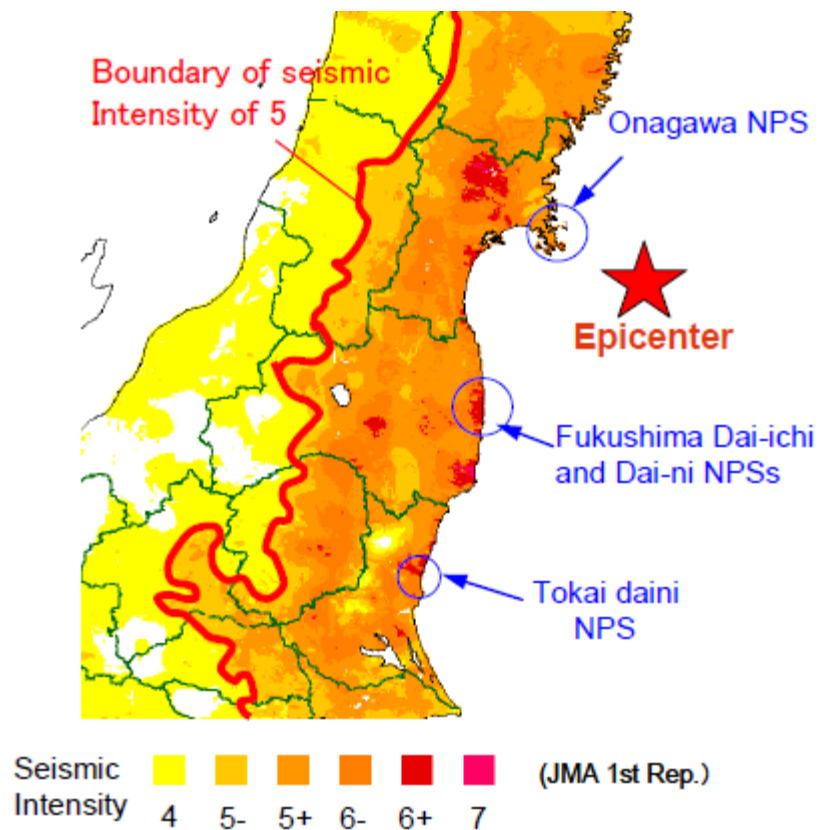


Fig. 4. Location of epicenter of the earthquake is shown with the resulting seismic intensity throughout Japan (Nuclear Emergency Response Headquarters GOJ, 2011).

On April 9th 2011, TEPCO reported that the initial tsunami arrived at about 15:27 Japan Standard Time (JST). According to the tide gauges the height of the tsunami was approximately 4 meters. The second major tsunami arrived at 15:35 JST but the water level was unknown because there was a tide gauge failure. The maximum scale of the tide gauge was 7.5 meters, so it was assumed the tsunami height was greater than 7.5 meters. An image released by TEPCO of the tsunami hitting the Fukushima NPS is shown in Fig. 5. Experts estimated that the tsunami height was more than 10 meters

(Nuclear Emergency Response Headquarters GOJ, 2011). The design at the Fukushima-Daiichi NPS did not contain seawalls high enough to prevent flooding from tsunamis of this magnitude. The earthquake caused damage to breakers and transmission lines for the Fukushima-Daiichi plant, which resulted in all external power supplies being lost for Units 1 thru 6. Along with external power supplies being lost from the earthquake all of the component cooling sea water pump facilities were flooded by the tsunami. The emergency diesel generators in the basements of Units 1 thru 5 were also flooded.



Fig. 5. Tsunami waves approaching the Fukushima Daiichi nuclear power plant, in a photo released by TEPCO (Nuclear Emergency Response Headquarters GOJ, 2011).

Prior to the earthquake on March 11th, 2011, Units 1-3 were operating at a constant power. At the time Unit 1 was operating with 400 fuel assemblies and had 392 fuel assemblies in its spent fuel pool. Unit 2 was operating with 548 fuel assemblies and had 615 fuel assemblies in its spent fuel pool. Unit 3 was operating with 548 fuel assemblies, 32 of which were MOX fuel assemblies. Units 4-6 were undergoing periodic inspections at the time and were disconnected from the power grid (Nuclear Emergency Response Headquarters GOJ, 2011).

The initial magnitude 9.0 earthquake quickly brought Units 1-3 into an automatic shutdown. Following the automatic shutdown the power generators were tripped, so the power supply for the NPS was switched to an off-site power supply. Even though the power supply was switched to off-site the NPS was not able to receive electricity because some of the transmission towers had collapsed, as a result of the earthquake. With no off-site power supply the NPS had to start the diesel generators to cool the reactors and spent fuel pools.

Once the tsunami hit all of the emergency generators for Units 1-5 became submerged. Without operating diesel generators the NPS lost all alternating current (AC) power for Units 1-5. TEPCO then opened up the isolation condensers (IC) system in Unit 1 and continued to inject fresh water into its shell side to maintain the IC functions. Units 2 and 3 were being cooled by the reactor core isolation cooling system (RCIC) as of March 12th, so the pressure and water levels at the time were stable in the primary containment vessels. In an attempt to recover the power supply for the units TEPCO requested emergency power supply vehicles. At 23:00 on March 11th it was confirmed

that radiation levels in the turbine building of Unit 1 were increasing. Soon after TEPCO acknowledged that the primary containment vessel may have exceeded its maximum operating pressure. Following Japan's Nuclear Emergency Preparedness Act TEPCO was ordered to reduce the pressure of Units 1 and 2. On March 12th at 5:46 TEPCO started to inject fresh water into Unit 1, along with preparing to perform pressure vents for the containment vessel. The high radiation levels in the reactor building were causing difficulties when trying to perform this task. Subsequently, a few hours after a pressure decrease was confirmed a hydrogen explosion occurred in the Unit 1 reactor building.

On March 12th at 11:36 the RCIC system for Unit 3 stopped and the high pressure core injection (HPCI) system was automatically turned on. Activation of the HPCI helped to maintain a constant water level in the reactor. At 2:42 on March 13th the HPCI system for Unit 3 stopped working, so TEPCO resorted to using fire engines to begin fresh water injection into the reactor along with pressure vents. The pressure was continuing to increase, so several vents were performed to decrease the primary containment vessel pressure. Even with several pressure vents at 11:01 on March 14th another hydrogen explosion occurred in the Unit 3 reactor building.

On March 14th it was determined that the water level was decreasing in Unit 2 because the RCIC had stopped. TEPCO began to try to reduce the pressure in the reactor pressure vessel and inject water into the vessel. At around 11:00 on March 13th the primary containment vessel had exceeded its maximum operating pressure. Subsequently, on March 15th at 6:00 JST another assumed hydrogen explosion occurred near the Unit 2 suppression chamber. Another hydrogen explosion also occurred in the

Unit 4 reactor building at around the same time as the Unit 3 explosion. On March 15th at 22:00, following regulations, TEPCO began to inject water into the Unit 4 spent fuel pool because cooling and water supplying functions were lost for the spent fuel pool.

The pressure in Unit 5, which also lost total AC power, was also increasing, but TEPCO was able to maintain the pressure and water level by injecting water into the reactor. Ultimately, TEPCO was able to bring Unit 5 to a cold shutdown at around 14:30 on March 20th. As for Unit 6, there were some effects pertaining to the earthquake and tsunami, but pressure and water levels were maintained. Pressure and water levels in Unit 6 were maintained because one of the diesel generators continued to operate.

Between the 6 reactor units there were 11 possible radiological releases between March 11th-23rd, in the form of explosions, pressure vents and fires (Mena, 2012). The direction of the release changed several times because of weather conditions, but the primary direction of the plume was to the northwest of the plant. The plume direction can be seen in Fig. 6. The Nuclear and Industrial Safety Agency (NISA) estimated that the total discharge from the Fukushima Daiichi plant was approximately 1.6×10^{17} Bq for ^{131}I and 1.5×10^{16} Bq for ^{137}Cs (Nuclear Emergency Response Headquarters GOJ, 2011).

Aerial Measuring Results

Joint US / Japan Survey Data

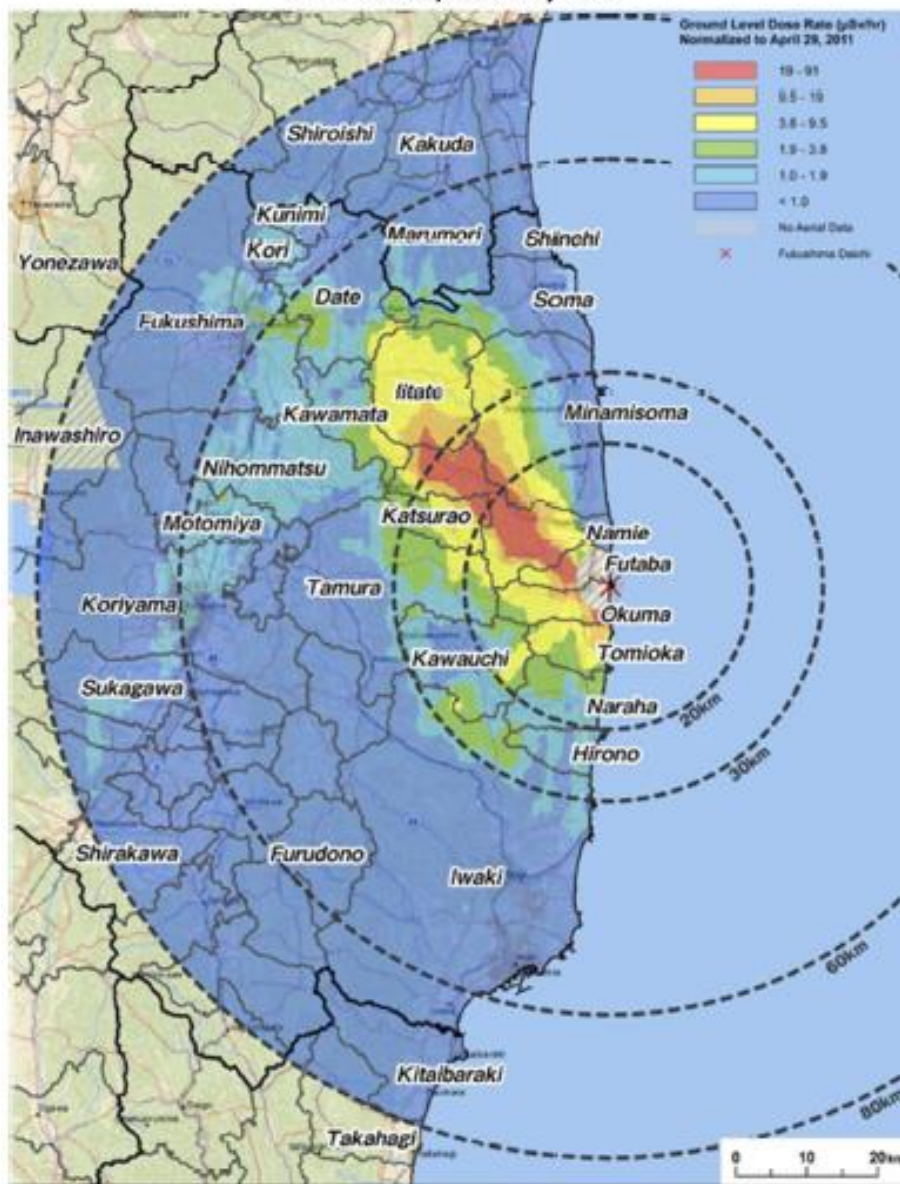


Fig. 6. Fukushima-Daiichi release plume from aerial measurements taken by U.S. and Japan teams (Reed, 2012).

In summary it was clear that a series of events led to the devastation at the Fukushima-Daiichi NPS. The accident was a direct result of the earthquake and ensuing tsunami that hit the NPS. The accident resulted in severe core damage for Units 1 through 3. Units 5 and 6 were able to successfully reach cold shutdowns without causing any damage to the reactors cores. Emergency response steps were taken to try to control the accident but the magnitude of the incident was overwhelming with the flooding and loss of power to many emergency and safety features.

Federal Radiological Monitoring and Assessment Center (FRMAC) Radiological Assessment Assumptions

When an incident such as Fukushima occurs one of the most important aspects of an effective nuclear/radiological emergency response is the radiological assessment process. The FRMAC, which acts as the hub for all data collected by responders, performs a concise analysis of the data from a radiological event. The main objective of a FRMAC assessment is to understand and interpret the radiological conditions and provide guidance to decision makers.

During exercises, and even the initial phases of a response, default assumptions are used for assessment calculations. These default assumptions are only used until data specific to the incident site are obtained for use. In the FRMAC Assessment Manual there are 10 specific default assumptions. These are:

1. Dose projections can include contributions from either two or four exposure pathways:
 - a. Two-Path Assessment involves the ground pathways:

- i. External exposure due to groundshine from deposited material from the release
 - ii. Inhalation due to resuspension of deposited material
 - b. Four-Pathway Assessment involves the plume and ground pathways:
 - i. External exposure due to groundshine from deposited material from the release
 - ii. Inhalation due to resuspension of deposited material
 - iii. External exposure due to being submersed in the passing plume
 - iv. Inhalation of radioactive material from the passing plume
- 2. The receptor is assumed to be in the plume, so the plume is assumed to be in contact with the ground.
- 3. Any material deposited by the passing plume is assumed to be immediately and completely deposited at the beginning of the passage of the plume
- 4. Noble Gas Dose Projections:

Radionuclides that are noble gases when released:

 - a. Are assumed to remain as gases during meteorological transport, even if they decay into a particulate daughter during the transport time
 - b. Are included in the external dose assessment from submersion in a plume
 - c. Are not assigned an inhalation dose coefficient, so they do not contribute to inhalation dose
 - d. Are not deposited on the ground, so they are not included in ground

pathway assessment calculations

- e. Noble gases that are daughters of ground-deposited radionuclides are assumed to remain on the ground and are not included in ground pathway assessment calculations.
5. The effects of radioactive decay, weathering and resuspension are included in the calculations.
6. All depositions are assumed to be dry particulates. Wet deposition due to increased localized deposition caused by rain or snow is not included
7. Dose from ingestion is not included in Public Protection Methods.
8. The receptor is:
 - a. An adult;
 - b. Outside in the contaminated area continuously without any protective measures;
 - c. Inhaling 1-micron Activity Median Aerodynamic Diameter (AMAD) particles in the lung class which provides the maximum dose.
 - i. Default inhalation dose coefficients and deposition velocities are used based on the assumed particle size. If actual particle size is known, this information is used.
9. The Bateman Equations are used to model the decay and in-growth of all radionuclides.
10. The FRMAC public protection methods generally assume the organ of interest is the whole body. Other organs may be evaluated against the Protective

Action Guidelines (PAGs) by utilizing organ-specific Dose Coefficients and PAGs.

During the exercises in which emergency response teams participate, the scenario and release parameters are well defined and fixed (Musolino, 2012). Assumptions are made about the plume, dose projections, radionuclide depositions and the receptors (Sandia National Laboratory, 2012). Along with the FRMAC Assessment Manual Default Assumptions, another main assumption during exercises is that the radionuclide deposition ratios will remain constant, only varying in terms of radioactive decay and weathering. This assumption is sometimes made regardless of large spatial and terrain variations.

During a radiological assessment for a reactor accident, two of the primary radionuclides of interest for radiological dose assessors are iodine and cesium. After a radiological incident the iodine isotopes, mainly ^{131}I , are the primary dose contributors for the first two months. After the iodine isotopes have decayed away, the main dose contributors are the cesium isotopes, specifically ^{137}Cs . All of the possible paths of exposure for these radionuclides are considered during a radiological assessment as shown in the Fig. 7. Responders try to collect data quickly after an accident, to better understand how the plume is travelling and how the radionuclides in the plume will deposit on the ground. Several factors contribute to how the radionuclides will travel, such as wind direction, precipitation, and properties of the radionuclides upon release.

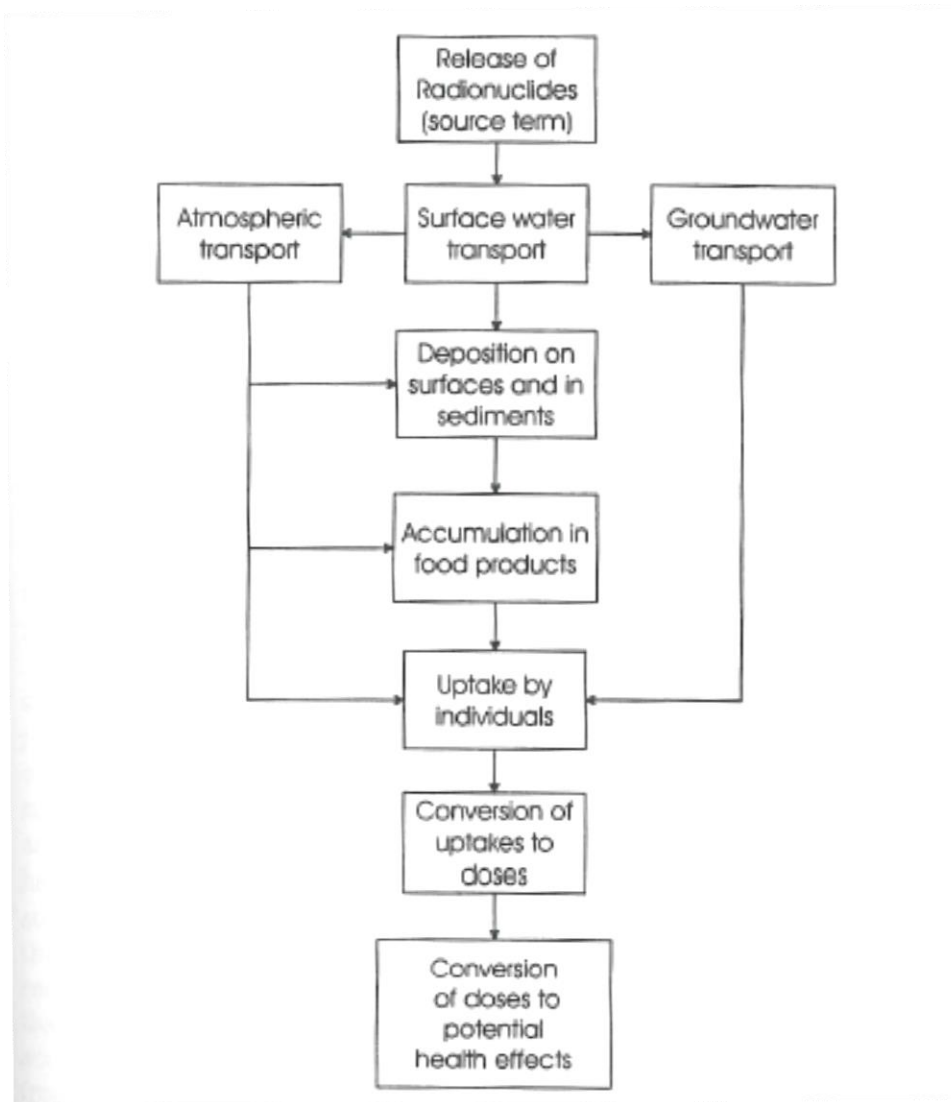


Fig. 7. Major steps in a radiological assessment [adapted from NCRP (1984a)] (Eisenbud, Merrill, Gesell, T., 1997).

With any radiological release from a reactor, many aspects need to be taken into account when it comes to the release of fission products and their behavior. The release of the fission products depends upon the chemical form, reaction and behavior in the primary system and the release location in the system. With the possibility of different release points, there becomes the possibility of many paths of travel. Many paths of travel means that there will also be different residence times and temperatures, which have an influence on the chemical reactions and the transport of the fission products. The path of travel for fission products through a reactor system is very complex since aerosols and volatile substances may deposit on walls or in pipes and be resuspended into the system. Homogenous and heterogeneous gas reactions can occur during the transport, which can considerably change the properties of the fission products. Gas reactions in turn can have an effect on the behavior of the fission products once they are released to the environment. So, from the initial release point to the final deposition point of fission products there are several factors that can affect deposition patterns, which can make a radiological assessment very complex for responders (Neeb, 1997). All of these factors contribute to the source term for the incident, one of the first estimates responders try to determine in the initial phases of a response.

Previous Research/Analysis

Literature pertaining to research done with respect to radionuclide deposition ratios is scarce. No literature was found specifically regarding radionuclide depositions of ^{131}I , ^{134}Cs , ^{136}Cs , and ^{137}Cs , from the Chernobyl accident. In the literature, it was noted that the radionuclide ratio of ^{131}I to ^{137}Cs varied spatially throughout Belarus. Analysis of

maps showed that the ^{131}I to ^{137}Cs ratio varied from approximately a factor of 5 to 10 throughout Belarus (NEA OECD, 2002). Yet, the ^{131}I to ^{137}Cs ratio was not studied over time in other countries after the Chernobyl accident. During the response to the Fukushima incident, analyses were performed pertaining to radionuclide distributions and concentrations using both air samples and *in situ* measurements.

After the accident an analysis of radionuclide ratios was performed using the Comprehensive Nuclear-Test Ban Treaty (CTBT) International Monitoring System (IMS). The IMS is comprised of four monitoring technologies for monitoring nuclear explosions of any kind. These technologies are: radionuclide, seismic, hydroacoustic, and infrasound. For the study after the Fukushima accident, the IMS stations in the U.S. for radionuclide monitoring were used. Radionuclide ratio data collected by the monitoring stations were used to compare data between stations and to show that the source of the radioactivity was from the Fukushima accident. The study was done to evaluate the overall capabilities of the system (Biegalski et. al., 2011).

The distance from the site of the accident to the closest U.S. IMS monitoring stations was over four thousand miles. Particulate measurements showed that iodine and cesium produced the highest number of detections at the particulate collection stations. The particulate collections at 10 of the monitoring stations showed that the $^{134}\text{Cs}/^{137}\text{Cs}$ ratio was relatively constant at ~ 1 over a period of about one month, as shown in Fig. 8. The $^{134}\text{Cs}/^{137}\text{Cs}$ ratio was expected to stay fairly constant for the first few months after the accident since the half-lives are 2.06 years and 30.2 years, respectively. The $^{136}\text{Cs}/^{137}\text{Cs}$ ratio was also studied over the same time period. The $^{136}\text{Cs}/^{137}\text{Cs}$ ratio varied between

the different IMS stations but followed an exponential decay overtime, because ^{136}Cs has a short half-life of 13 days, compared to the half-life of ^{137}Cs . The trend for $^{136}\text{Cs}/^{137}\text{Cs}$ is shown in Fig. 9.

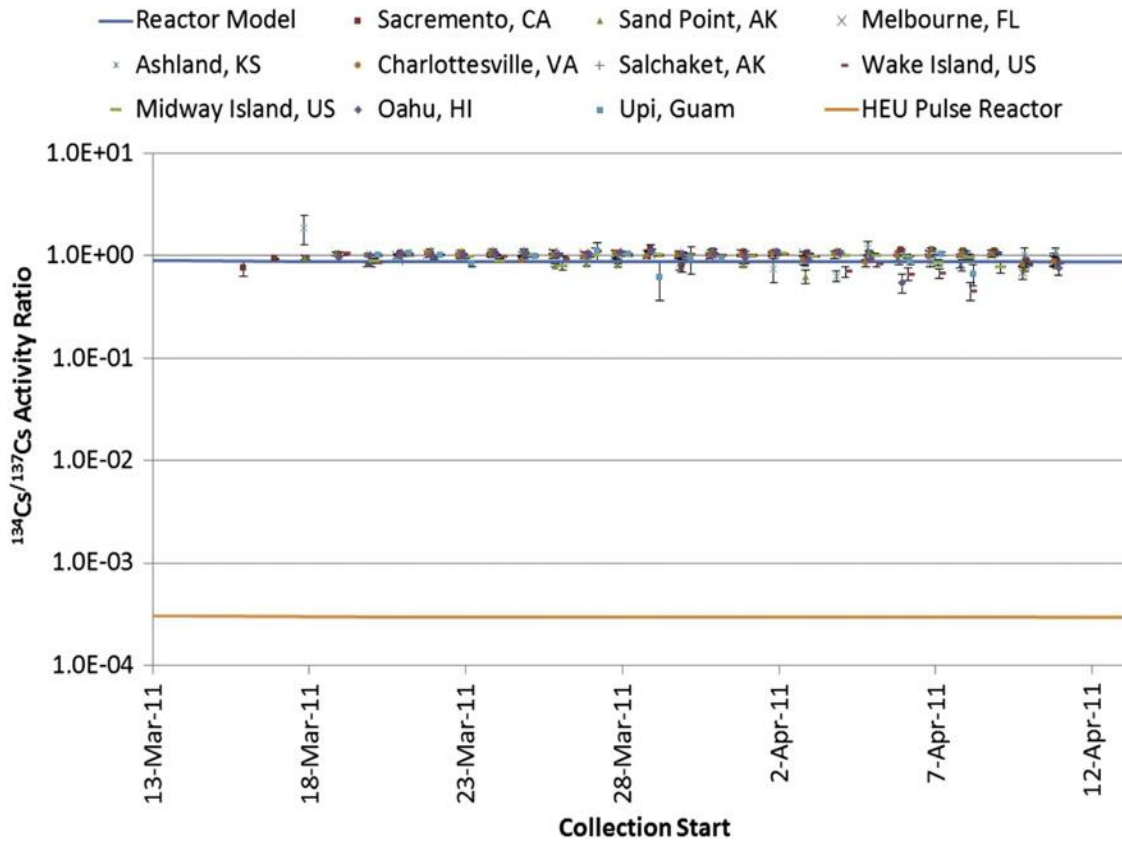


Fig. 8. $^{134}\text{Cs}/^{137}\text{Cs}$ isotopic activity ratio for US IMS stations (1σ error bars) (Biegalski et. al., 2011).

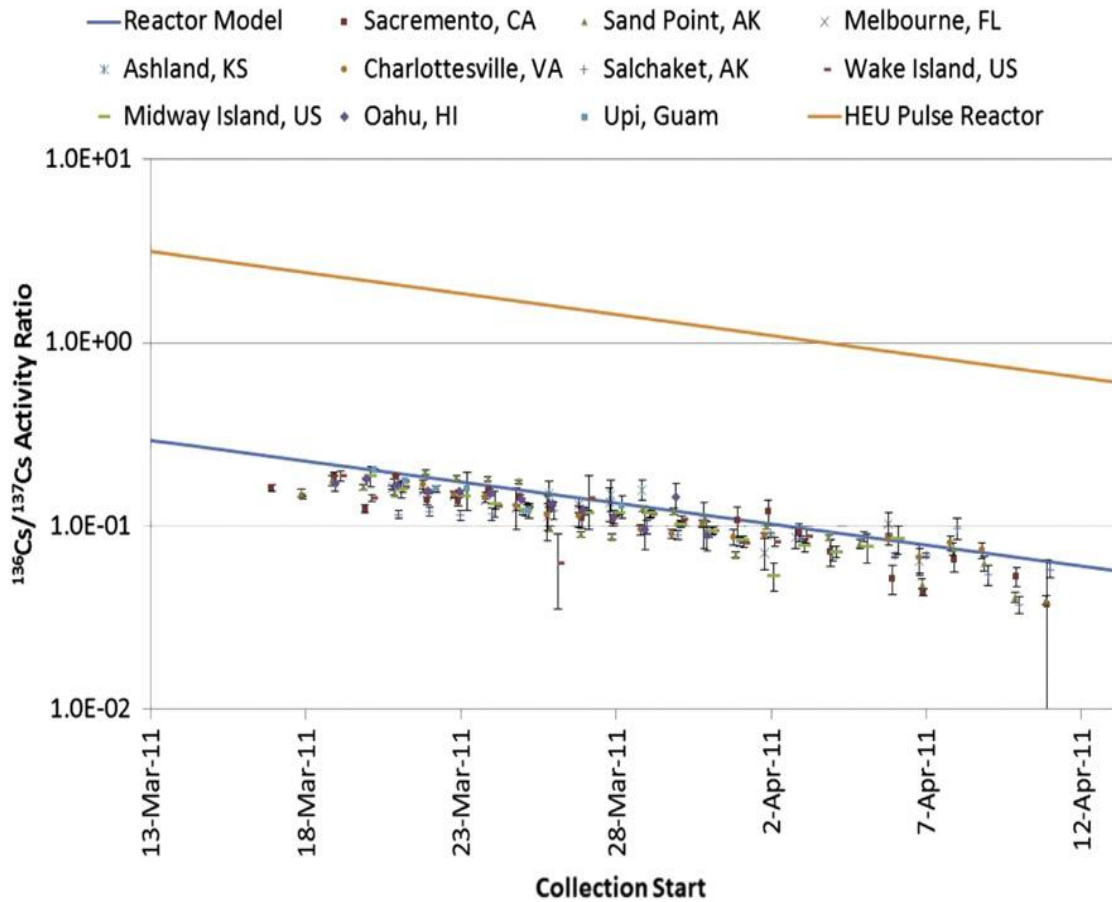


Fig. 9. $^{136}\text{Cs}/^{137}\text{Cs}$ isotopic activity ratio for US IMS stations (1σ error bars) (Biegalski et. al., 2011).

The U.S. IMS study shows that the travel of radionuclides such as cesium and iodine should not cause the concentration ratios to vary greatly. Though the travel of the radionuclides may not affect the concentration ratios in air samples this does not mean that the radionuclide concentration ratios will not change when the radionuclides deposit.

An analysis was also performed for data from the early stages of the response in

March, with respect to the two rainfall events that took place in Japan. Contour maps for the radionuclide depositions throughout east-central Japan are shown in Fig. 10. Two rain events occurred in March on the 15-16th and the 21st. The amount of rainfall was based on the Automated Meteorological Data Acquisition System (AMeDAS), which is a high resolution surface observation network developed by the Japan Meteorological Agency (JMA). AMeDAS is used to gather regional weather data to help verify forecast performance. According to the AMeDAS continual rainfall occurred between 1700 hours on March 15 and 0400 hours on March 16 in the northern Fukushima Prefecture. The next rain event occurred between 0800 hours on March 21 and 0600 hours on March 23 in the Ibaraki, Chiba, Tochigi, and Saitama prefectures and in Tokyo (Kinoshita et al., 2011). The contour maps for the rain events are shown in Fig. 11.

The contour maps from Fig. 10 show that throughout Japan the radionuclide depositions were varying spatially. It can be seen that there was an increase in the activity of several radionuclides to the northwest of the plant. There was also a clear increase in the $^{131}\text{I}/^{137}\text{Cs}$ ratio to the south-southwest of the plant. The region to the south-southwest of the plant was one of the areas of Japan which received an increase in precipitation as seen in Fig. 11. This analysis shows that depositions of certain radionuclides will vary throughout an area, especially if there is an increase in precipitation.

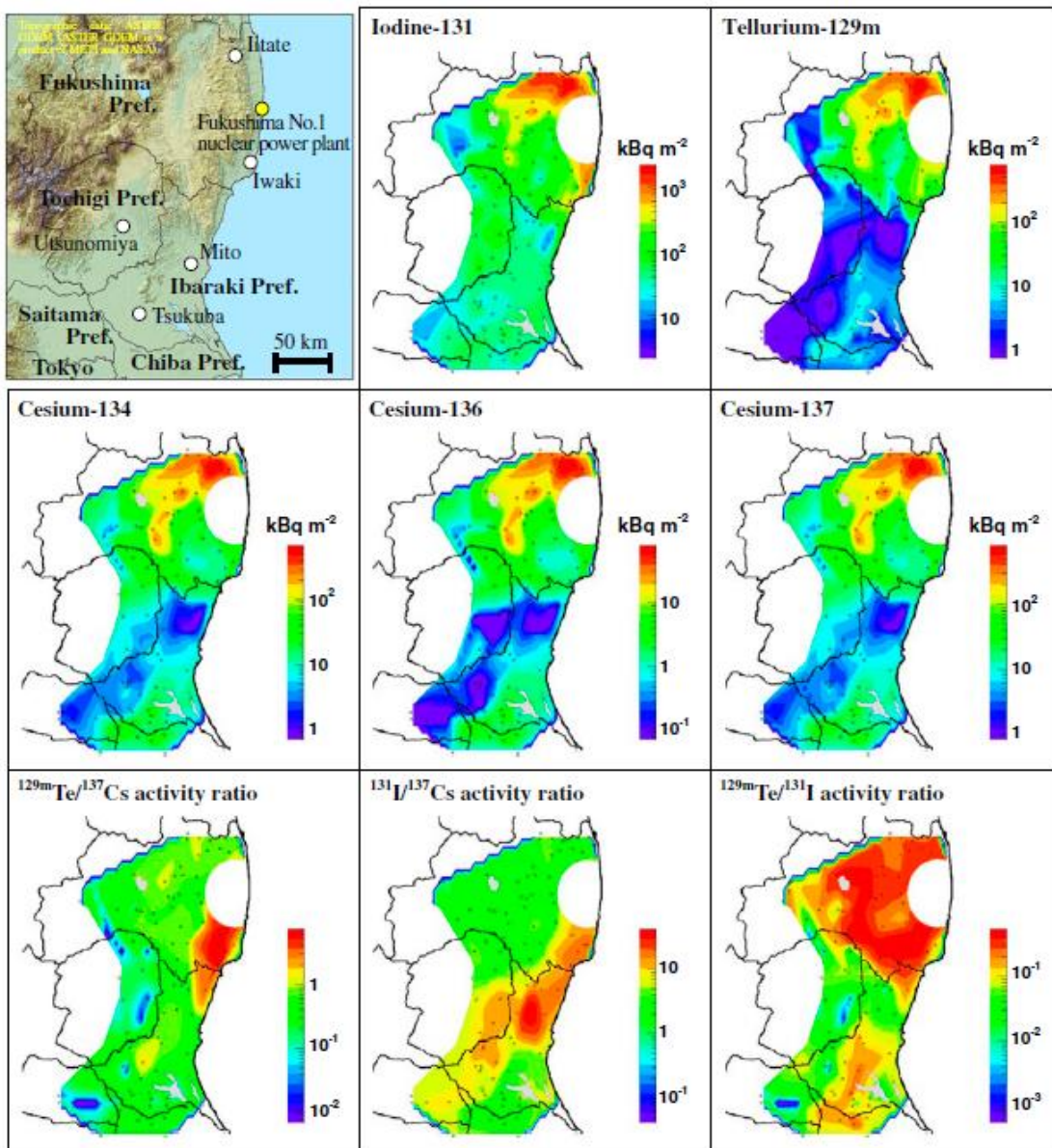


Fig. 10. Contour maps of depositions for several radionuclides; and activity ratios for $^{129\text{m}}\text{Te}/^{137}\text{Cs}$, $^{131}\text{I}/^{137}\text{Cs}$, and $^{129\text{m}}\text{Te}/^{131}\text{I}$ through Japan are shown. Activities from March 29th, 2011 are shown. (Kinoshita et. al., 2011)

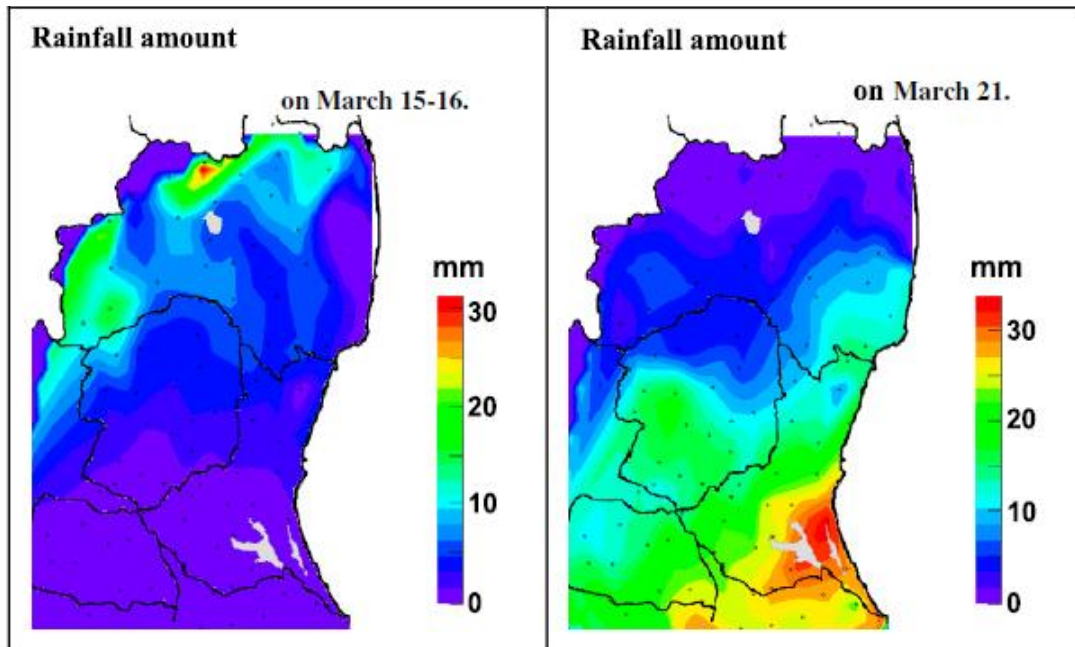


Fig. 11. Amount of rainfall in Japan on March 15-16th and March 21, based on AMeDAS (Kinoshita et. al., 2011).

While in Japan the DOE/NNSA CMRT and other response teams evaluated the radiological situation using *in situ* measurements, soil and air samples. To determine the consistency of the radionuclide mixture from the release the activity ratios for ^{134}Cs to ^{137}Cs were followed for 158 *in situ* measurements and 174 air samples (Musolino et. al., 2012). The analytical results of the *in situ* measurements and air samples are shown in Fig.12 and Fig. 13, respectively (Musolino et. al., 2012). The $^{134}\text{Cs}/^{137}\text{Cs}$ ratio was very consistent for both the air and *in situ* samples, maintaining a ratio of ~ 1 . The concentrations of ^{134}Cs and ^{137}Cs did vary throughout Japan but the ratio of ^{134}Cs to ^{137}Cs did not vary (Musolino et. al., 2012). A consistent ratio for ^{134}Cs to ^{137}Cs was

expected for the first few months after the release because the half-lives of both of these radionuclides are long compared to the time frame of the data set.

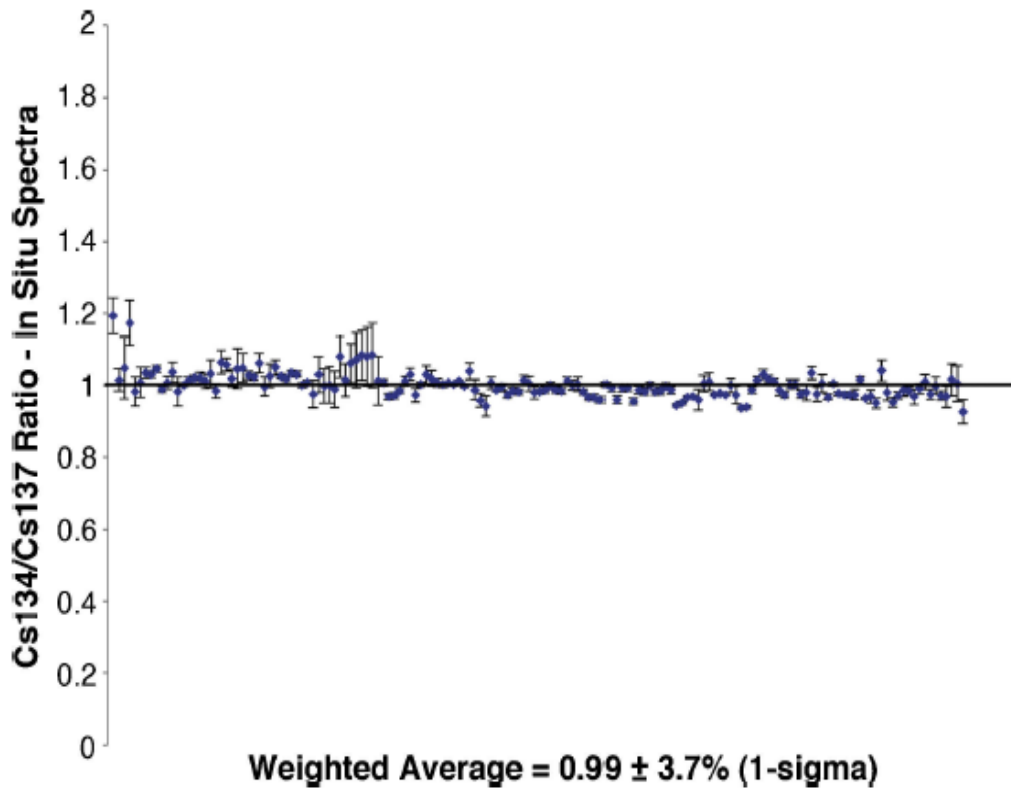


Fig. 12. $^{134}\text{Cs}/^{137}\text{Cs}$ activity ratios for 158 *in situ* measurements. Figure courtesy of Lawrence Livermore National Laboratory (Musolino et. al., 2012).

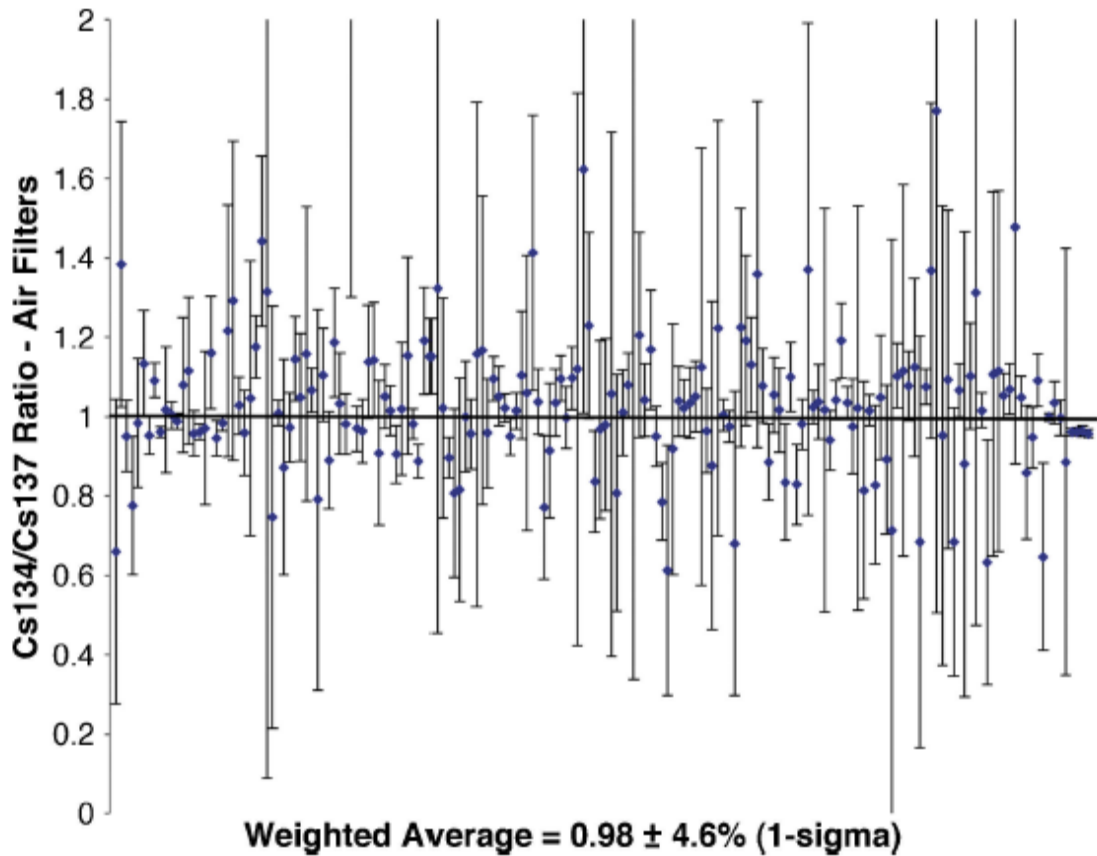


Fig. 13. $^{134}\text{Cs}/^{137}\text{Cs}$ activity ratios for 174 air samples. Figure courtesy of Lawrence Livermore National Laboratory (Musolino et. al., 2012).

Both the CMRT and the DOD collected data in Japan. The CMHT performed an analysis of the cesium/iodine ratio with data collected around the U.S. Embassy/Tokyo area, the CMRT field samples and the DOD measurement data. The sampling periods for the CMRT and DOD data were March 20-26 and March 13-25, respectively. The ratio comparison for the U.S. Embassy/Tokyo area, CMRT field samples and DOD

measurement data are shown in Table 3. The original comparison was for ^{134}Cs and ^{137}Cs to total iodine but for Table 3 the ratios were inverted to show the $^{131}\text{I}/^{137}\text{Cs}$ ratio.

Table 3. Iodine/ ^{137}Cs ratio and its associated standard deviation are given for data from CMRT and DOD data.

Data Source	Iodine/ ^{137}Cs	STD (\pm)
Embassy/Tokyo	45.45	27.03
Field Samples	29.41	21.74
DOD	7.14	8.33

The research reported here focuses on the analysis of spectra from the *in situ* measurements made by the CMRT along with measurements made by representatives of the GOJ after departure of the CMRT. The literature review shows that analyses of radionuclide depositions were performed by the CMRT. But these analyses were performed with data sets of less than 200 measurements from the early phases of their response in Japan. This research discussed here consists of a larger data set, which is necessary for an effective analysis. In this research, analysis of the *in situ* measurements was conducted to ascertain whether the infield assumptions the U.S. response teams made were valid during a real-life response.

METHODS AND MATERIALS

DOE/NNSA CMRT Data

The field measurements taken in Japan by the CMRT were used to perform the radionuclide deposition analysis for this research. All of the data collected by the CMRT were stored in the DOE Radiological Assessment and Monitoring System (RAMS). In total there were approximately 250,000 data files within RAMS from the Fukushima response. For the purpose of the research only the *in situ* measurement data were extracted. There were 292 *in situ* measurement data files, which included raw spectra, collection date, sample number, sample instrument, field team, latitude, longitude, sampling time, live time, exposure rate and measurement height. Not every file had the complete information but all of the spectra were identified with the collection date and associated latitude and longitude. Latitude and longitude were necessary to determine the spatial variations in the radionuclide deposition ratios. All of the information for the *in situ* measurements was consolidated into a spreadsheet and each associated spectrum was analyzed using the Ortec GammaVision® software. A peak analysis was performed on each spectrum to determine the net counts under each photopeak of interest. Peak analysis was performed for the following radionuclides; ^{134}Cs , ^{136}Cs , ^{137}Cs and ^{131}I . Each radionuclide has one or more photons associated with its decay, so the photon with the highest branching ratio for each radionuclide was used for the peak analysis. The associated gamma-ray energies and branching ratios for the radionuclides used were: 604 keV (97.6%), 818 keV (100%), 662 keV (84.62%) and 364 keV (81.24%), respectively.

The net counts under the photopeak for each radionuclide was recorded along with their associated uncertainty. The net counts and uncertainties were input into the same spreadsheet with all of the measurement information, and deposition ratios were calculated. The ratios were calculated for ^{134}Cs , ^{136}Cs and ^{131}I relative to ^{137}Cs . These ratios allowed comparison of all of the radionuclide depositions to each other at specific locations. When calculating the ratios, the uncertainties for the net counts for each photopeak were propagated to determine the uncertainty of the deposition ratios. In addition to comparing the deposition ratios to each other, they were also compared to the values shown in Table 4. This table was obtained from the FRMAC Assessment Manual Volume 3, which gave isotopic ratios for a LWR core-damage accident. The table gives the concentration of thirty-nine radionuclides relative to ^{137}Cs for specific times after the shutdown of a LWR. The values from this table were compared against the calculated values because the values in the table accounted for decay of deposited radionuclides after a reactor shutdown. This allowed the data obtained at Fukushima to be compared to the FRMAC values since the Fukushima reactors were shut down after the initial earthquake.

Table 4. Radionuclide concentrations relative to ^{137}Cs for a LWR core-damage accident are given for specific times after reactor shutdown. (Sandia National Laboratory, 2003).

Radionuclide to ^{137}Cs Ratio Time After Shutdown								
Radionuclide	1 hr	6 hr	12 hr	24 hr	3 days	7 days	15 days	30 days
^{132}Te	12.2	11.7	11.1	10.0	6.5	2.8	0.5	0.0
^{131}I	18.1	17.7	17.4	16.6	14.0	9.9	5.0	1.4
^{132}I	23.7	14.5	11.8	10.3	6.7	2.9	0.5	0.0
^{133}I	35.6	30.1	24.7	16.5	3.3	0.1	0.0	0.0
^{135}I	30.3	17.9	9.6	2.7	0.0	0.0	0.0	0.0
^{134}Cs	1.6	1.6	1.6	1.6	1.6	1.6	1.6	1.6
^{136}Cs	0.6	0.6	0.6	0.6	0.5	0.4	0.3	0.1
^{137}Cs	1.0	1.0	1.0	1.0	1.0	1.0	1.0	1.0

The deposition ratios for $^{136}\text{Cs}/^{137}\text{Cs}$ and $^{131}\text{I}/^{137}\text{Cs}$ could only be compared to the values in Table 4 for periods between one and two weeks after the shutdown of the reactors because the first spectrum collected by the CMRT used for this research was collected on 17 March 2011, approximately one week after shutdown. The first *in situ* measurement spectrum did not show the presence of ^{136}Cs or ^{137}Cs , so it was not used. The first spectrum used was collected on 20 March 2011, which was a little over a week from the shutdown of the reactors.

The deposition ratios from *in situ* measurements on 20 March 2011 for $^{136}\text{Cs}/^{137}\text{Cs}$ and $^{131}\text{I}/^{137}\text{Cs}$ were averaged to represent the concentrations of ^{136}Cs and ^{131}I , relative to ^{137}Cs for comparison to the FRMAC values, one week after shutdown. The deposition ratios represent *in situ* measurements taken about nine days after initial reactor shut down. The data set used did not contain *in situ* measurements from exactly one week

after shut down, which is why the deposition ratios from about nine days after shut down were used for comparison. In order to make the comparison at two weeks for ^{136}Cs , the $^{136}\text{Cs}/^{137}\text{Cs}$ ratios for *in situ* measurements taken between the 25th and 29th were averaged. Data from several days had to be averaged to represent the ratio for two weeks, because only one *in situ* measurement showed the presence of ^{136}Cs on the 25th, which is exactly two weeks after reactor shutdown. The $^{131}\text{I}/^{137}\text{Cs}$ ratios from *in situ* measurements taken on the 25th were averaged to represent the ^{131}I ratio for two weeks after shutdown. The average ratios of $^{136}\text{Cs}/^{137}\text{Cs}$ and $^{131}\text{I}/^{137}\text{Cs}$, approximately one and two weeks after shut down, were used to compare to the concentrations given in Table 4.

In Table 4, the concentration of ^{134}Cs relative to ^{137}Cs is not expected to change even 30 days after shutdown, because the half-lives of both cesium isotopes are much longer than 30 days. For the ^{134}Cs ratio all the values were averaged from 20 March 2011 to 2 July 2011. The average values for the $^{134}\text{Cs}/^{137}\text{Cs}$, and the average values for $^{136}\text{Cs}/^{137}\text{Cs}$ and $^{131}\text{I}/^{137}\text{Cs}$, one and two weeks after shutdown, were compared to the values in Table 4 to determine how closely they related. Next, all of the calculated deposition ratios over the whole data set time frame were plotted as a function of time, to determine whether or not the respective decay rates were followed.

To visualize the locations of the *in situ* measurements throughout Japan, ESRI software ArcMap 10.1 was utilized. These plots provided the exact locations of the *in situ* measurements and allowed determination of the location of hot spots. The software produced maps were compared to NNSA aerial monitoring results and National Atmospheric Release Advisory Center (NARAC) simulations to determine if the trends

of the *in situ* measurements followed the path of the plume. Mapping and analyzing these data made it simple to determine whether or not the deposition ratios were varying spatially throughout Japan.

Digital elevation model (DEM) data for Japan (United States Geological Survey, 2013) were also used to obtain a better visualization of the changes in elevation throughout Japan. This information aided in determining whether elevation changes had more of a significant impact on the deposition of particulates like cesium or more volatile radionuclides such as iodine.

JAEA ^{134}Cs and ^{137}Cs Variation Data

Cesium *in situ* measurement data acquired by the GOJ were also analyzed. These data consisted of four different data sets at the same location for many locations throughout Japan. There was the second measurement, third prophase (before typhoon season) measurement, third anaphase (after typhoon season) measurement, and fourth measurement.¹ The second measurement consisted of 1016 *in situ* measurements taken between 14 December 2011 and 28 May 2012. The third prophase measurement consisted of 387 *in situ* measurements taken between 13 August 2012 and 19 September 2012. The third anaphase measurement included 380 measurements taken between 5 November 2012 and 12 December 2012. The fourth measurement included 382 *in situ* measurements taken between 13 June 2013 and 10 July 2013.

Using the GOJ ^{134}Cs and ^{137}Cs variation data, the $^{134}\text{Cs}/^{137}\text{Cs}$ ratio was calculated for the specific measurement locations. Once the cesium ratios were calculated for each data

¹ Prophase and anaphase in this case refer to the distribution of seasons in Japan.

set, the data were plotted according to the measurement date to determine if there were any fluctuations with the cesium ratio. The data were also plotted using ESRI software ArcMap 10.1 to obtain an idea of the spatial locations of the *in situ* measurements throughout Japan. If there were any fluctuations with the cesium data, mapping the data would help to determine the locations in Japan in which there may have been higher or lower cesium deposition ratios. The calculated ^{134}Cs deposition ratio was also compared to the FRMAC Assessment Manual value in Table 4.

The average of the ratios for each measurement set (second, third prophase, third anaphase, fourth) was calculated and decay corrected to determine if the deposition ratios were the same as the NNSA data at the time of those measurements.

RESULTS

DOE/NNSA CMRT Data

The $^{134}\text{Cs}/^{137}\text{Cs}$ Deposition Ratios

When comparing the analyzed DOE/NNSA CMRT data to the FRMAC Assessment Manual Vol. 3 values in Table 4 there were some clear differences. According to Table 4, the $^{134}\text{Cs}/^{137}\text{Cs}$ ratio should maintain a value of 1.6 up to 30 days after reactor shutdown. The value calculated from the CMRT data was 1.047 ± 0.051 . These values are different but the CMRT data did show that ^{134}Cs and ^{137}Cs maintained a relatively constant ratio even 30 days after reactor shutdown. Figure 14 shows the trend of the $^{134}\text{Cs}/^{137}\text{Cs}$ ratio for the whole CMRT *in situ* measurement data set. Figure 15 also shows that there were approximately 20 data points that deviated from the mean. These data points represent measurements with count rates comparable to background for both cesium isotopes. Analysis showed that the uncertainties were greater than 20%, because of the lack of counts under the photopeaks. The low count rates could be attributed to short detector live times or significant plume deposition may not have occurred at the time of the measurements. The live times for the measurements varied from 300-1800 seconds. Though detector live times of 1800 seconds were not used until 22 May 2011, when the GOJ started to take the *in situ* measurements. All of the measurements that produced high uncertainties (>20%) for the $^{134}\text{Cs}/^{137}\text{Cs}$ ratio were from the Tokyo region of Japan, which was over 200 km from the accident site. The significant plume travel distance and plume depletion during travel are reasonable explanations for these low-activity measurements. Figure 15 shows a map of Japan with the *in situ* measurement

locations marked along with the highlighted $^{134}\text{Cs}/^{137}\text{Cs}$ data points in the Tokyo region that had high uncertainties.

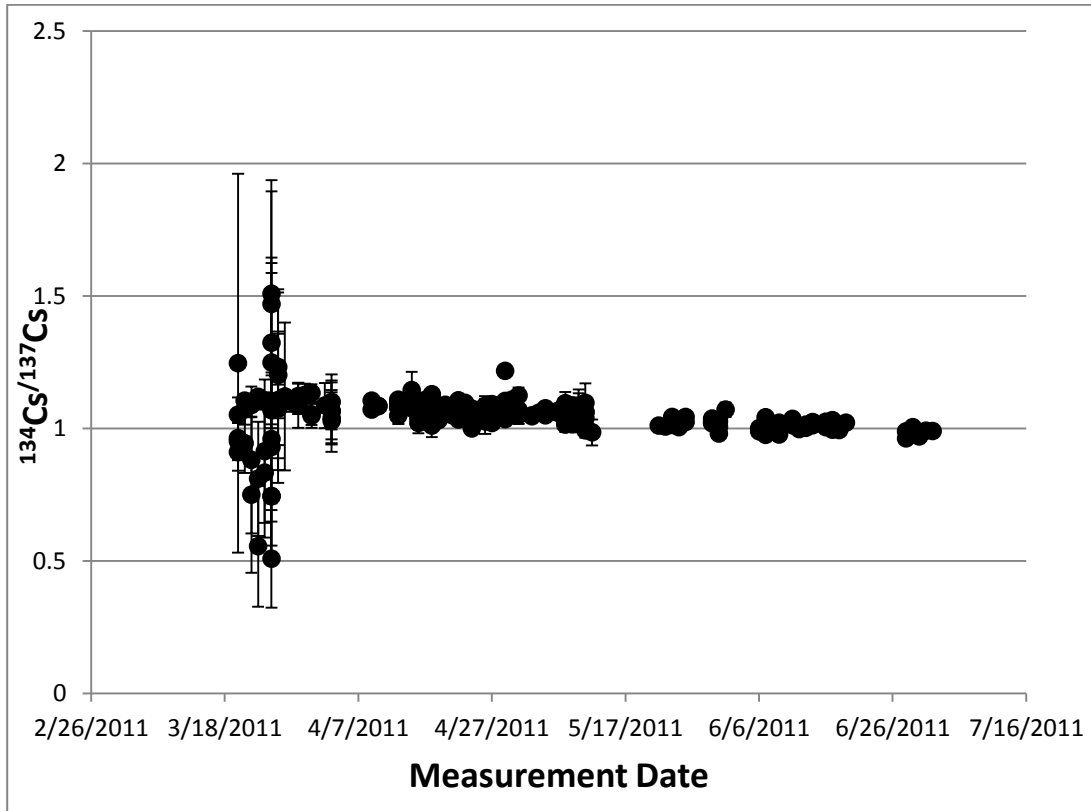


Fig. 14. $^{134}\text{Cs}/^{137}\text{Cs}$ net counts ratio with respect to the date the measurements were taken.

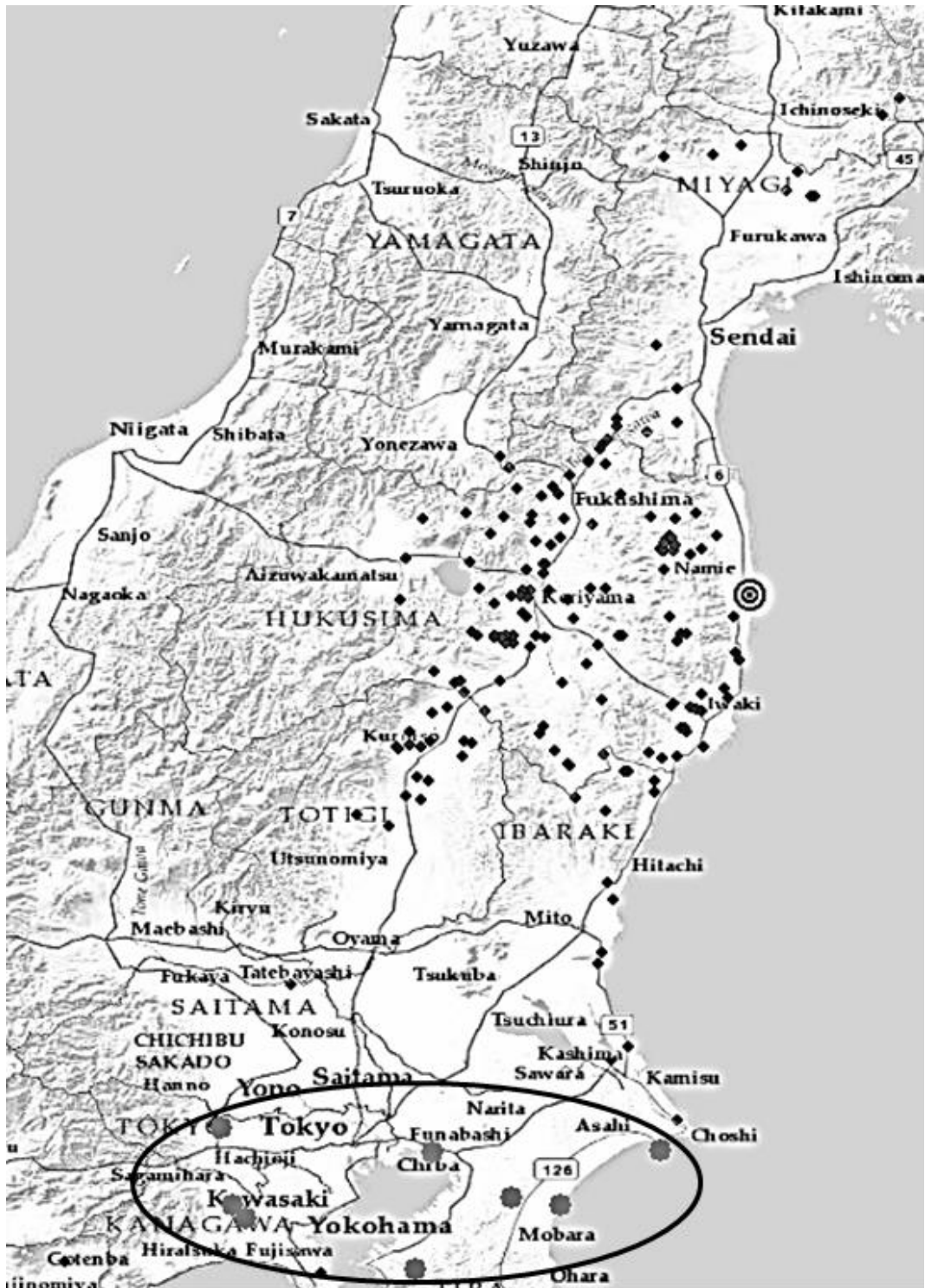


Fig. 15. Map displaying *in situ* measurement locations with highlighted locations for the $^{134}\text{Cs}/^{137}\text{Cs}$ values with uncertainties greater than 20%.

The $^{136}\text{Cs}/^{137}\text{Cs}$ Deposition Ratios

The data for $^{136}\text{Cs}/^{137}\text{Cs}$ when plotted showed a relatively fast exponential decay as seen in Fig. 16, because the half-life of ^{136}Cs is only 13 days. There were 7 out of 191 data points that deviated from the curve but these data points had relatively high uncertainties that varied from 17-62%. The data collected by the CMRT covered about 64,000 km² of Japan, which was useful when determining spatial variance of the data points. The curve for $^{136}\text{Cs}/^{137}\text{Cs}$ showed that the ^{136}Cs deposition ratio should not vary much even with respect to large spatial and terrain variations, much like $^{134}\text{Cs}/^{137}\text{Cs}$. Approximately one week after reactor shutdown the deposition ratio for ^{136}Cs was about 0.13 ± 0.018 , which does differ from the value of 0.4 given in Table 4. The analyzed *in situ* measurement data produced ^{136}Cs ratios consistently lower than the FRMAC values in Table 4.

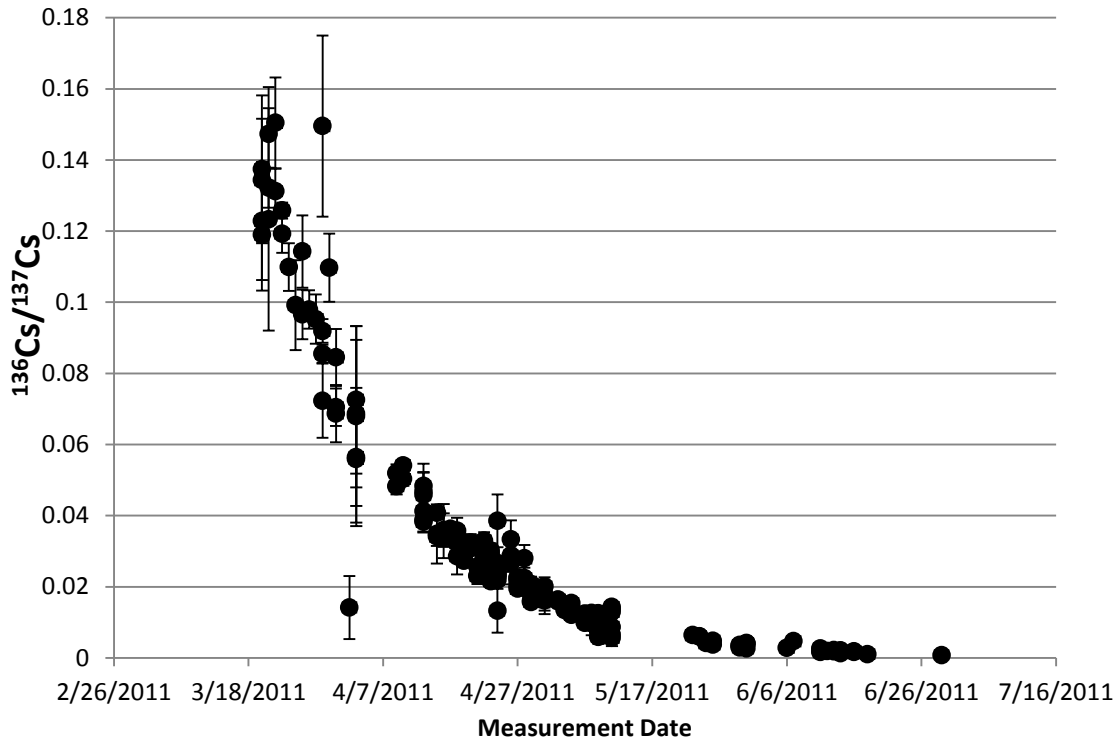


Fig. 16. $^{136}\text{Cs}/^{137}\text{Cs}$ net counts ratio with respect to the date the measurements were taken.

The $^{131}\text{I}/^{137}\text{Cs}$ Deposition Ratios

The $^{131}\text{I}/^{137}\text{Cs}$ data also followed an exponential decay as seen in Fig. 17 but the data fluctuated. The $^{131}\text{I}/^{137}\text{Cs}$ deposition in the early days of the response showed ratios significantly higher than expected. Table 4 shows that the ^{131}I ratio should be 18.1 approximately 1 hour after shutdown, yet the collected data shows ^{131}I ratios as high as 53.56 ± 2.68 , over a week after shutdown. The high values from the $^{131}\text{I}/^{137}\text{Cs}$ data set were marked on a map to better show their location. The map is shown on Fig. 18 and all the high values appear to be towards the southwest of the nuclear power plants. During

the incident on 14 March 2011 when the Unit 3 explosion occurred, the wind direction had changed to the SSW of the plants (Blumenthal, 2012). Unit 3 was also operating with 548 fuel assemblies, including 32 MOX fuel assemblies (Nuclear Emergency Response Headquarters GOJ, 2011). It is unknown whether or not the percentage of MOX fuel would contribute to the deposition ratios being as high as they were in the area.

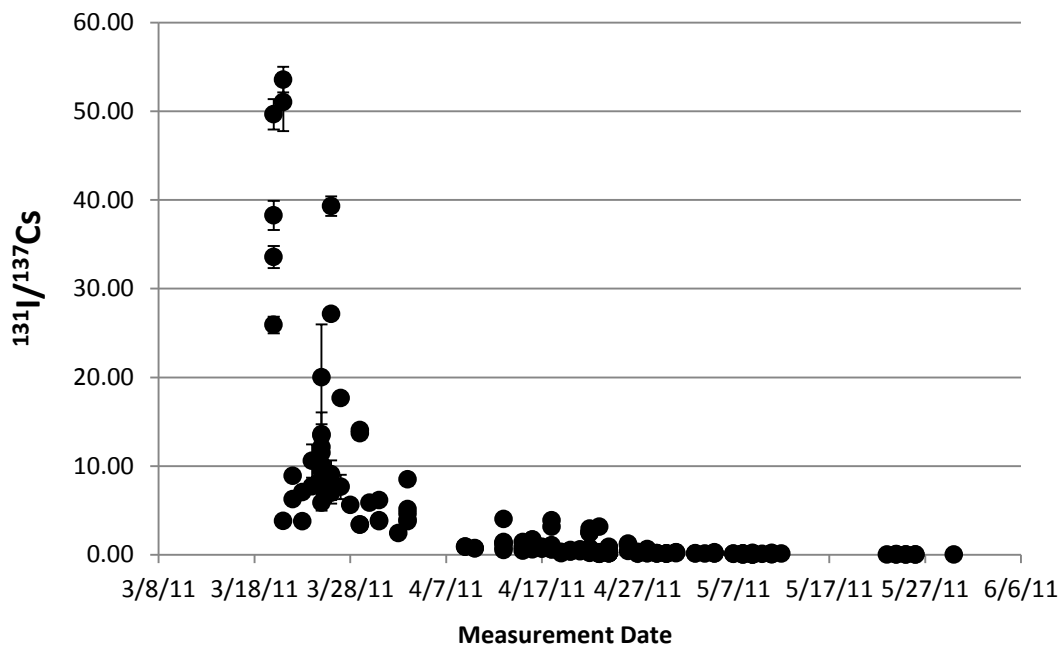


Fig. 17. $^{131}\text{I}/^{137}\text{Cs}$ net counts ratio with respect to the date the measurements were taken.

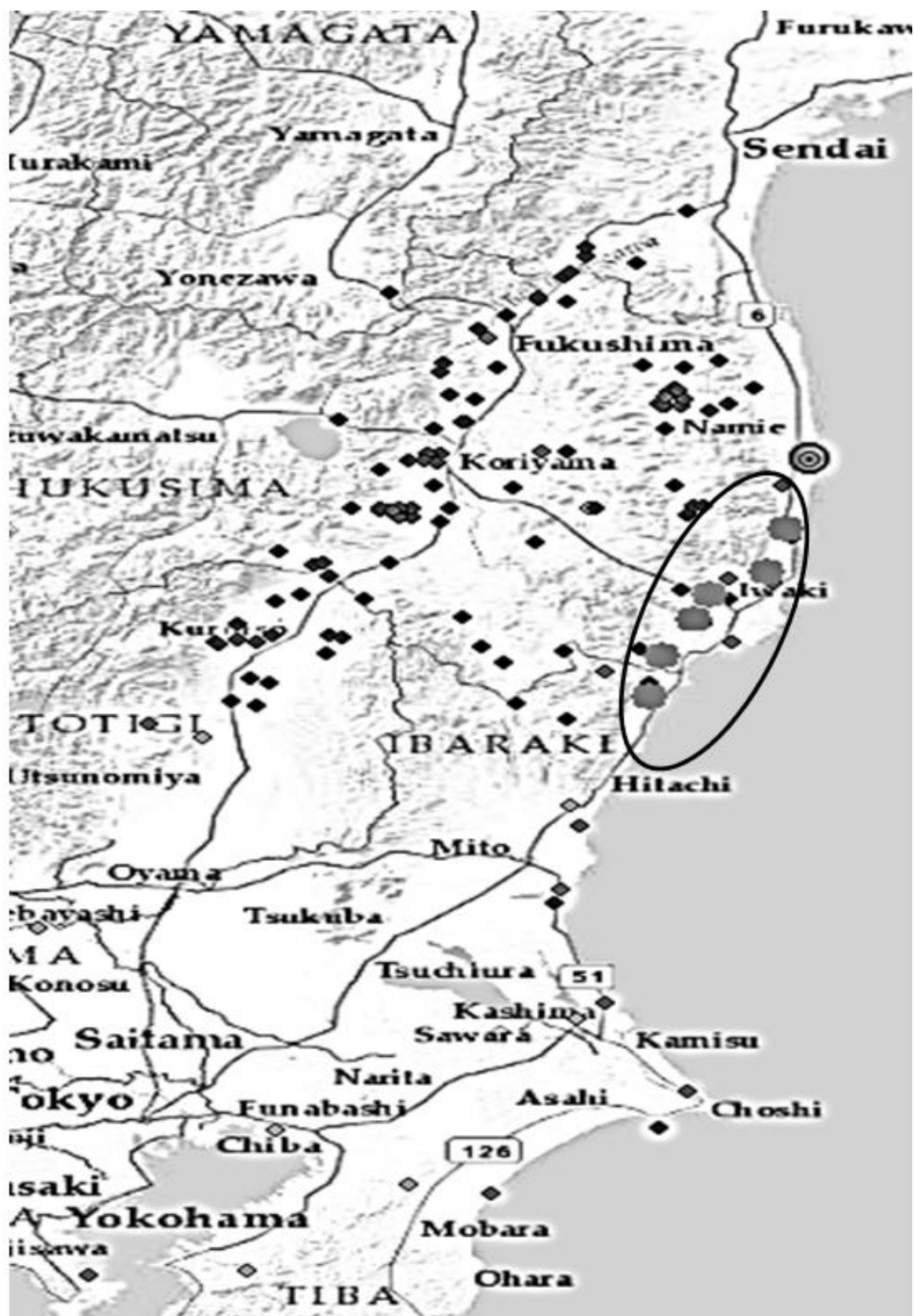


Fig. 18. Map displaying *in situ* measurement locations with highlighted locations for highest $^{131}\text{I}/^{137}\text{Cs}$ values.

**Comparing FRAMC Assessment Manual Vol. 3 Values to DOE/NNSA Fukushima
in situ Measurements**

Comparing the calculated values from Table 5 to the FRMAC Assessment Manual Vol. 3 values in Table 4 reveals some clear differences, especially with the $^{131}\text{I}/^{137}\text{Cs}$ concentration. The average value of $^{134}\text{Cs}/^{137}\text{Cs}$ ratio for the data set and the average value of the $^{136}\text{Cs}/^{137}\text{Cs}$ ratio for 1 and 2 weeks after shutdown were lower than the values from Table 4. As for the $^{131}\text{I}/^{137}\text{Cs}$ data, the calculated averages were higher than the values in Table 4. Most of the high $^{131}\text{I}/^{137}\text{Cs}$ values were to the southwest of the nuclear power plants. These high values have been provided in Table 6. There are many factors that could possibly contribute to the differences in the values from Table 4 and Table 5. The precipitation in Japan was considered to be the primary cause of depositions differences but elevation at the measurement sites was also considered.

Table 5. Average ratios and standard deviations for the deposition ratios of interest ($^{134}\text{Cs}/^{137}\text{Cs}$, $^{136}\text{Cs}/^{137}\text{Cs}$, $^{131}\text{I}/^{137}\text{Cs}$) with respect to different times after shutdown.

	$^{134}\text{Cs}/^{137}\text{Cs}$	σ	$^{136}\text{Cs}/^{137}\text{Cs}$	σ	$^{131}\text{I}/^{137}\text{Cs}$	σ
Average	1.047	0.09	0.033	0.0338	3.80	8.73
Average 1 week after shutdown	1.024	0.12	0.128	0.0077	36.85	8.61
Average 2 week after shutdown	1.052	0.30	0.100	0.0204	11.10	3.60

Table 6. The highest $^{131}\text{I}/^{137}\text{Cs}$ values located to the southwest of the nuclear power plants are given along with their associated uncertainty, latitude and longitude.

Measurement Date:	Latitude	Longitude	$^{131}\text{I}/^{137}\text{Cs}$	Uncertainty (%)
3-20-2011	37.235578	140.985693	49.65	3.43
3-20-2011	37.001973	140.812589	38.26	4.31
3-20-2011	36.903004	140.751618	25.90	3.58
3-20-2011	36.797261	140.726352	33.57	3.66
3-21-2011	37.124803	140.947787	53.56	2.68
3-21-2011	37.067582	140.838236	51.03	6.41

JAEA ^{134}Cs and ^{137}Cs Variation Data

The *in situ* measurement data that the JAEA collected were not compared to the FRMAC values, because the collection date was past 30 days after reactor shutdown. The JAEA data were used to determine whether or not the $^{134}\text{Cs}/^{137}\text{Cs}$ concentration ratio would change over longer time periods, for reasons other than radioactive decay.

The second measurement consisted of 1016 *in situ* measurements taken between 14 December 2011 and 28 May 2012. The location of all 1016 *in situ* measurements are shown in Fig. 19. The $^{134}\text{Cs}/^{137}\text{Cs}$ concentration ratio average for the measurements was 0.78 with a standard deviation of 0.04. When the ratio was decay corrected to the time of the initial reactor shutdown a $^{134}\text{Cs}/^{137}\text{Cs}$ concentration ratio of 1.06 was calculated. The

decay corrected value of 1.062 was not far from the average concentration ratio of 1.047 calculated from the CMRT data. The decay corrected values for the $^{134}\text{Cs}/^{137}\text{Cs}$ concentration ratios for the third prophase, third anaphase, and fourth measurements were 1.068, 1.069, and 1.062, respectively. All of the data did not have associated measurement errors, so errors were not propagated when calculating the concentration ratios. The $^{134}\text{Cs}/^{137}\text{Cs}$ concentration ratio averages and decay corrected averages for all four measurements are in Table 7. The data in Table 7 shows that even two years after an accident the cesium concentration ratio will remain constant only changing as a result of radioactive decay. Maps of the locations of all the *in situ* measurements and plots of the data for the second, third prophase, third anaphase, and fourth measurements are in Appendix A.

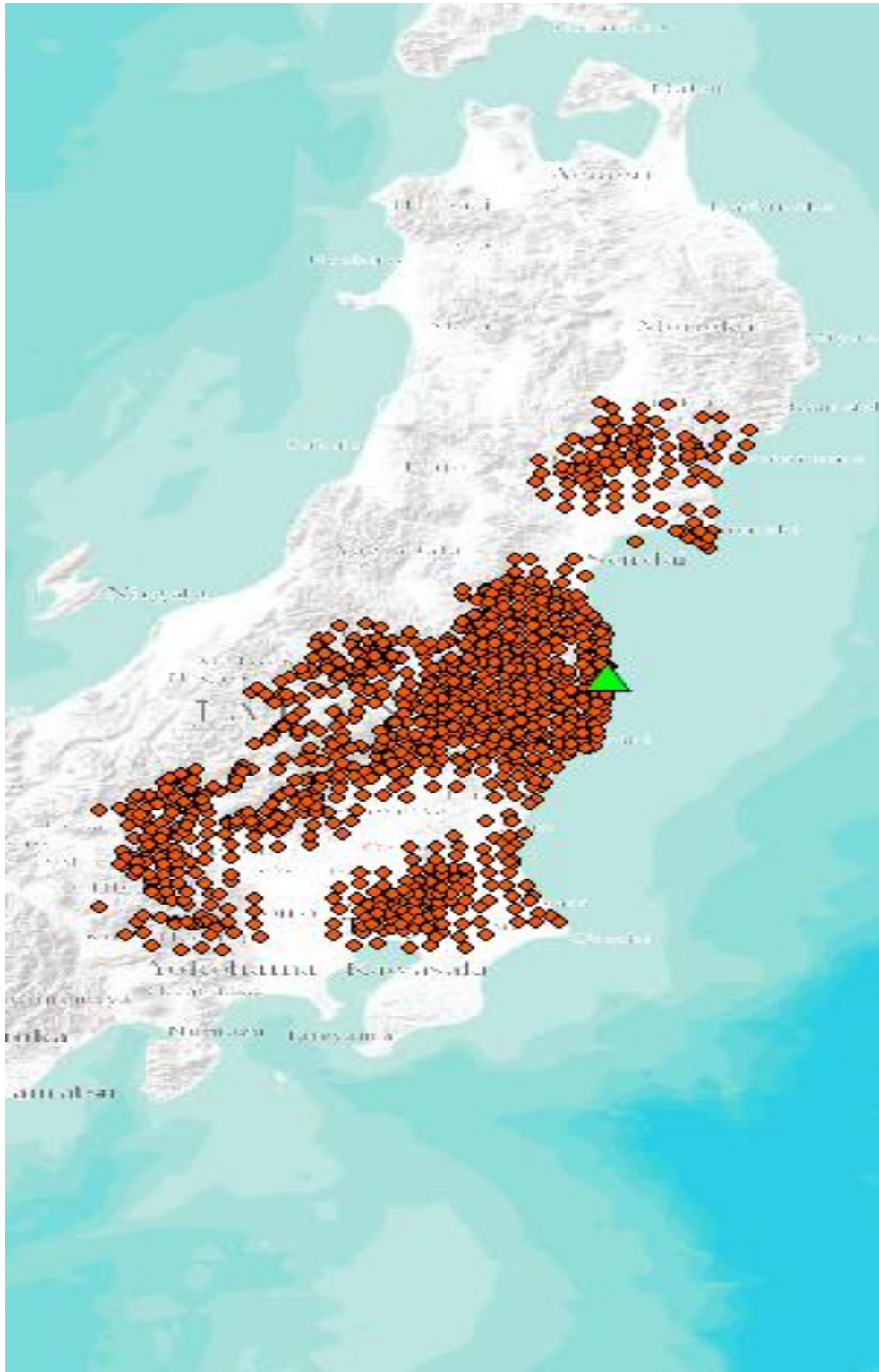


Fig. 19. Location of the 1016 *in situ* measurements for the 2nd measurement.

Table 7. Average and decay corrected average of $^{134}\text{Cs}/^{137}\text{Cs}$ concentration ratio from JAEA data.

Measurement	# of Measurements	Average $^{134}\text{Cs}/^{137}\text{Cs}$ concentration ratio	Standard Deviation	Decay Corrected Average $^{134}\text{Cs}/^{137}\text{Cs}$ concentration ratio
2nd Measurement	1016	0.7819	0.0369	1.062
3rd Prophase Measurement	387	0.6611	0.0305	1.068
3rd Anaphase Measurement	380	0.6156	0.0295	1.069
4th Measurement	383	0.5104	0.0238	1.062

DISCUSSION

When comparing the values in Table 5 and Table 6, it should be noted that there are differences between the FRMAC Manual Vol. 3 LWR reactor core damage scenario and the Fukushima-Daiichi Incident. The Fukushima-Daiichi Incident included severe core damage to several boiling water reactors. Along with the core damage of several reactors there were also a number of releases after shutdown. The FRMAC scenario was based on a 1000 MW_e LWR with core damage and a prompt release. Release fractions for the scenario were averaged for both pressurized-water reactors (PWR) and boiling water reactors (BWR). The FRMAC scenario also assumed that all depositions were dry (Sandia National Laboratory, 2003).

The FRMAC reactor core damage scenario was similar to an emergency response exercise that may take place, which is why the values in Table 4 were used despite the scenario differences. The values from Table 4 and data acquired from the Fukushima incident were not expected to match exactly because of the scenario differences. The Table 5 values were used to determine whether or not there would be extreme differences in the assumed depositions from exercises and actual accident depositions. The data from Fukushima for ¹³⁴Cs/¹³⁷Cs and ¹³⁶Cs/¹³⁷Cs showed no extreme differences and followed their expected decay curves over time. With respect to the cesium ratios, the values from assumptions made in exercises and trainings should not differ greatly from an actual accident scenario. The data for ¹³¹I/¹³⁷Cs, however, shows that other possible considerations should be made during exercises and trainings for more volatile radionuclides such as iodine.

Data gathered during the incident showed that wet depositions in Japan during the incident did have a significant effect on the final deposition pattern (NARAC. Private Communication. 25 October 2013). The increased precipitation throughout Japan may have been the cause of the increased deposition ratios for $^{131}\text{I}/^{137}\text{Cs}$ to the southwest of Fukushima-Daiichi. It also appeared as though the high depositions to the southwest were located at low elevation along the coastline. The location of the *in situ* measurements along with the Digital Elevation Model (DEM) can be seen in Fig. 20. The lighter portions of the DEM are areas where the elevation is higher than sea level and the darker portions are where elevation is closer to sea level. White dots on the map indicate the highest deposition ratios for $^{131}\text{I}/^{137}\text{Cs}$. Based on a Lagrangian integrated trajectory model, HYSPLIT, the plume from the NPP had an altitude of 0-1000 meters and stayed in the Fukushima prefecture at 1700 hours on the 15th of March. The plume also stayed in the Ibaraki and Chiba prefecture at 1100 hours on the 21st of March. The plume stayed in these regions before the rain events that occurred so most of the radionuclides in the air were washed out by the precipitation. The increased $^{131}\text{I}/^{137}\text{Cs}$ deposition ratios to the southwest of the NPP could have possibly been caused by particulate material being blocked by the mountainous areas at higher elevations. The more volatile radionuclides such as ^{131}I appeared to have been more easily transported than the particulates, such as ^{137}Cs , in the mountainous area (Kinoshita et. al., 2011). The blockage of the particulates along with precipitation in the region seems to be the most probable cause for why the $^{131}\text{I}/^{137}\text{Cs}$ deposition ratios were higher at the lower elevations to the southwest of the NPP.

Another possible cause of the increase in the $^{131}\text{I}/^{137}\text{Cs}$ deposition ratios is the fallout of cesium particulates, over the ocean. When the plume travelled off the coast the particulates could have deposited off the coast and the remaining iodine and cesium could have been deposited along the coastline to the southwest of the NPP, when the plume returned over land. Another possibility that has not yet been validated is that the increased iodine deposition ratios to the southwest could be a direct result from the release of one specific reactor. Unit 3 was operating with 32 MOX fuel assemblies, which would cause a slight difference in the amount of fission products in the fuel, but as mentioned before it is unknown whether or not the percentage of MOX fuel would contribute to the deposition ratios being as high as they were in the area.

Deposition distance from the plant was also considered as a possible factor for an increased deposition ratio for $^{131}\text{I}/^{137}\text{Cs}$. Initially, it was assumed that more iodine would deposit further away from the plant than cesium, since iodine is a reactive gas and cesium is more of a particulate. The *in situ* measurements did not show any correlation with respect to iodine and direct distance from the plant. For this reason, distance from the plant appears to have had no effect on the deposition of iodine and cesium in Japan. It was determined that whether the measurement location was on a wet, dry, disturbed, undisturbed or paved area could have an effect on the depositions (Musolino, 2012). The surface and atmospheric conditions can cause deposition rates to vary by a factor of 20 or more for elements such as iodine and cesium (Sandia National Lab, 2003). Detailed environmental conditions at the measurement locations were not included in the data set. This information would have been helpful when trying to consider all of the conditions

at the specific measurement locations. Field notes such as these along with a larger data set would be necessary to determine the causes of fluctuations in the data. Without the measurement location information, it could not be determined if environmental conditions were the cause of the increased deposition of iodine to the southwest of the plant.

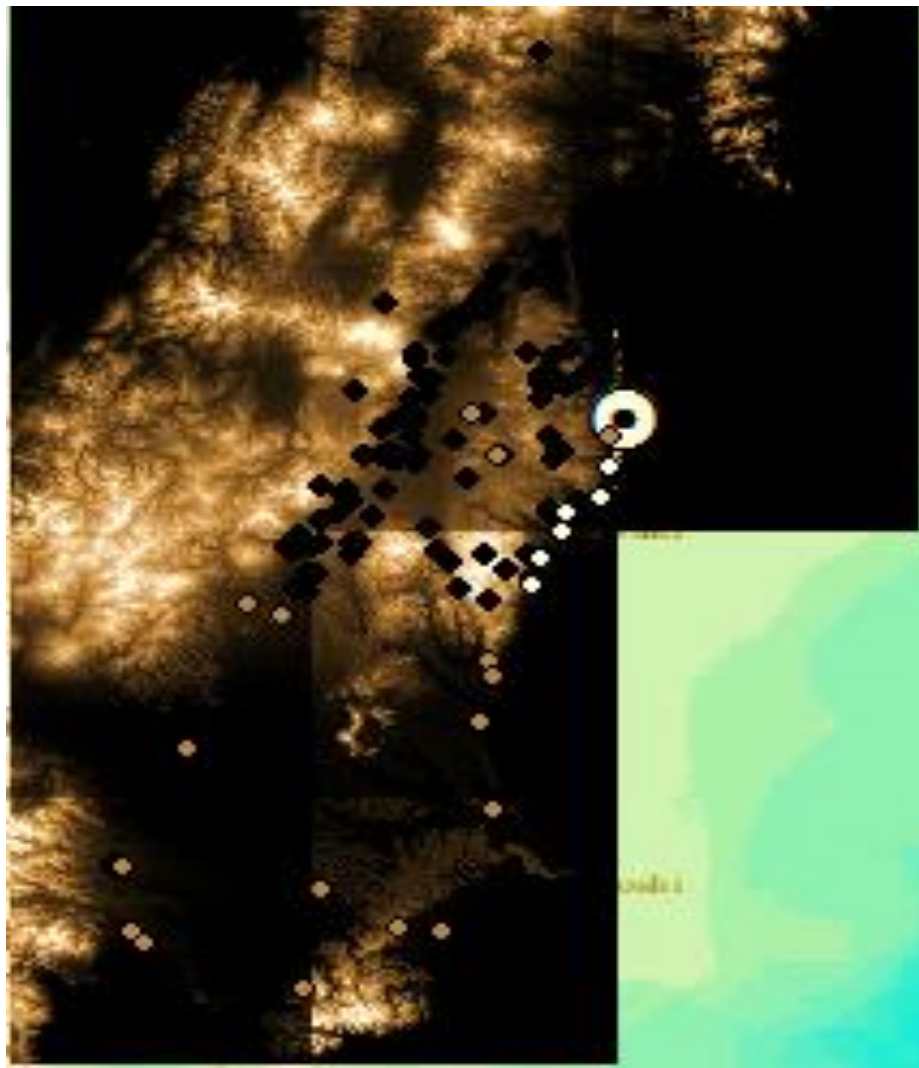


Fig. 20. Map of Japan with *in situ* measurement locations and DEMs.

The ^{134}Cs and ^{137}Cs variation data from the JAEA helped to confirm what was observed with the $^{134}\text{Cs}/^{137}\text{Cs}$ concentration ratio with the CMRT data. When the $^{134}\text{Cs}/^{137}\text{Cs}$ concentration ratios from the second, third prophase, third anaphase, and fourth measurements were decay corrected, the results were within ~ 0.2 of the average ratio from the CMRT data. The CMRT *in situ* measurement data set was relatively small, so a more robust data set of 2166 *in situ* measurements aided with confirming that the $^{134}\text{Cs}/^{137}\text{Cs}$ ratio overtime would remain constant only changing with respect to radioactive decay.

CONCLUSIONS

From the analysis of the NNSA data and the conditions in Japan at the time of the incident, it is clear that many factors contribute to the final deposition patterns of radionuclides. Assumptions that emergency response workers make in the initial stages of accidents and during exercises seem to be valid for radionuclides such as cesium. The NNSA and JAEA data consisted of 5 data sets that were collected over a period of ~2.33 years. Even though the measurements were taken at different times over this period, the $^{134}\text{Cs}/^{137}\text{Cs}$ ratio remained constant only appearing to change as a result of radioactive decay. The $^{134}\text{Cs}/^{137}\text{Cs}$ ratio at the beginning of the response and the decay corrected ratios from the later measurements stayed between 1.04-1.06, which can be claimed as a constant ratio. The assumption of interest for this research was that radionuclide deposition ratios will remain constant, only varying in terms of radioactive decay and weathering. This assumption is at times made regardless of large spatial and terrain variation. But since the data set covered such a large spatial area of Japan consisting of many terrain variations the data set really helped to validate the assumption of interest specifically for the $^{134}\text{Cs}/^{137}\text{Cs}$ ratio.

The data set for the $^{136}\text{Cs}/^{137}\text{Cs}$ consisted of only 192 *in situ* measurements, but did show a consistent exponential decay. Though there was a clear exponential decay a larger data set covering a larger area of Japan would be needed to confirm whether or not the $^{136}\text{Cs}/^{137}\text{Cs}$ ratio would remain constant, only changing as a result of radioactive decay. The data for $^{136}\text{Cs}/^{137}\text{Cs}$ would need to be obtained within the first 50 days after the accident because the half-life of ^{136}Cs is relatively short at 13 days, so 50 days after

the Fukushima incident ^{136}Cs would be difficult to detect compared to ^{134}Cs and ^{137}Cs .

While the $^{134}\text{Cs}/^{137}\text{Cs}$ ratio helped to validate the assumption of interest, the $^{131}\text{I}/^{137}\text{Cs}$ ratio did not. The $^{131}\text{I}/^{137}\text{Cs}$ data showed that not every radionuclide will deposit and only vary in terms of radioactive decay and weathering. The $^{131}\text{I}/^{137}\text{Cs}$ ratios during the earlier stages of the response were significantly higher than expected in some areas of Japan. Ratios towards the SSW of the NPP were as high as 53.56, yet the FRMAC Assessment Manual says that one hour after reactor shutdown the ratio should only be about 18.1. With the small data set and the results for the $^{131}\text{I}/^{137}\text{Cs}$ ratio, it cannot be said for sure whether or not the emergency response training and exercise assumption of interest is valid. Based on the data, and without a larger data set at this time, it must be said that the assumption of interest for the $^{131}\text{I}/^{137}\text{Cs}$ ratio is not valid during a response with changing weather conditions.

The data set that was analyzed for the purpose of this research was small. During the research there was a continuous search for *in situ* measurement data, with associated latitude, longitude and measurement information. Yet, no other complete data sets were found at the time. More data must be analyzed to be able to reach a conclusion on the validity of the assumption that the radionuclide deposition ratios will remain constant, only varying in terms of decay and weathering. Several data sets were examined, such as *in situ* measurement data from the Ministry of Education, Culture, Sports, Science & Technology in Japan (MEXT) and International Atomic Energy Agency (IAEA). Most of the data found did not have the associated latitudes and longitudes, which were a necessary part of the research plan. The data that was used in this research, taken by the

DOE/NNSA CMRT, was the best overall data set found.

Further research is needed in order to determine the validity of the assumption of interest, if sufficient *in situ* measurement data are found. For the purpose of further research a robust *in situ* measurement data set from Japan, which has the associated latitude and longitude, measurement time, dead time and preferably the raw spectra from the *in situ* measurements, would be needed. During the research it also became clear how important information such as, measurement location conditions, elevation and precipitation data were when analyzing *in situ* measurement data. A data set with all of this information would allow for a more informative data analysis allowing for the consideration of spatial differences and several environmental conditions.

It should be noted that the assumptions made during exercises and responses are conservative initially for simplicity before more information on the incident is known, such as the source term. Regardless, training and exercise assumptions could possibly be adjusted or changed to have responders better prepared in case of an incident of this magnitude, should these conditions occur again.

REFERENCES

1. Biegalski, S.R., Bwoyer, T.W., Eslinger, P.W., Friese, J.A., Greenwood, L.R., Haas, D.A., Hayes, J.C., Hoffman, I., Keillor, M., Miley, H.S., Moring, M. Analysis of Data from Sensitive U.S. Monitoring Stations for the Fukushima Dai-ichi Nuclear Reactor Accident. *Journal of Environmental Radioactivity* 114 15-21; 2011.
2. Blumenthal, D. Introduction to the Special Issue on the U.S. Response to the Fukushima Accident. *Health Phys.* 102(5): 482-484; 2012.
3. Eisenbud, Merrill, Gesell, T. *Environmental Radioactivity from Natural, Industrial, and Military Sources* 4th Edition, New York: Academic Press; 1997.
4. Federal Emergency Management Agency (FEMA), National Incident Management System [online]. Available at: <http://www.fema.gov/national-incident-management-system>. Accessed 28 January 2014.
5. Federal Emergency Management Agency (FEMA), National Response Framework Information Sheet. 1 May 2013. Available at: <http://www.fema.gov/national-response-framework>. Accessed February 2014.
6. Federal Emergency Management Agency (FEMA), Nuclear/Radiological Incident Annex. June 2008. Available at: https://www.fema.gov/pdf/emergency/nrf/nrf_nuclearradiologicalincidentannex.pdf Accessed January 2014.
7. Marianno, C. Emergency Response Health Physics Module 1, NUEN 689 lecture notes at Texas A&M University, February 2014.
8. Marianno, C. United States Response Assets, NUEN 689 lecture notes at Texas A&M University, February 2014.
9. Marianno, C. Private Communication. 2 December 2013.

10. Mena, R, Pemberton W, Beal W. Emergency Response Health Physics. *Health Phys.* 102(5): 542-548; 2012.
11. Mena, R. Private Communication. 23 July 2013.
12. Musolino, S, Clark, H, McCullough, T, Pemberton, W. Environmental Measurements in an Emergency: This Is Not a Drill. *Health Phys.* 102(5): 516-526; 2012.
13. Musolino, S. Private Communication. 18 July 2013.
14. Musolino, S. Private Communication. 13 July 2013.
15. Neeb, K. *The Radiochemistry of Nuclear Power Plants with Light Water Reactors*, New York: Walter de Gruyter; 1997.
16. N. Kinoshita, K. Sueki, K. Sasa, J. Kitagawa, S. Ikarashi, et al. Assessment of Individual Radionuclide Distributions from the Fukushima Nuclear Accident Covering Central-east Japan. *Proceedings of the National Academy of Sciences* 109 (49) 2011[online]. Available at: www.pnas.org/cgi/doi/10.1073/pnas.1111724108. Accessed 17 February 2014.
17. Nuclear Emergency Response Headquarters GOJ. Report of the Japanese Government to the IAEA Ministerial Conference on Nuclear Safety – The Accident at TEPCO’s Fukushima Nuclear Power Stations. June 2011. Available at: <http://www.iaea.org/newscenter/focus/fukushima/japan-report>. Accessed January 2014.
18. Nuclear Energy Agency (NEA) Organization for Economic Co-operation and Development (OECD). *Chernobyl Assessment of Radiological and Health Impacts, 2002 Update of Chernobyl: Ten Years On*. OECD Publications Printed in Paris, France 2002. Available at: <https://www.oecd-nea.org/rp/chernobyl/>. Accessed March 2014.

19. Nuclear Energy Institute. Fact Sheet Comparing Chernobyl and Fukushima; 2011
Available at: <http://www.nei.org/Master-Document-Folder/Backgrounders/Fact-Sheets/Japan-Comparing-Chernobyl-And-Fukushima>. Accessed February 2014.
20. Organization for Economic Co-operation and Development (OECD). Nuclear Legislation in OECD Countries, Regulatory and Institutional Framework for Nuclear Activities, Japan. 2011 Available at: <https://www.oecd-nea.org/law/legislation/japan.pdf>. Accessed February 2014.
21. Organization for Economic Co-operation and Development (OECD). Nuclear Legislation in OECD Countries, Regulatory and Institutional Framework for Nuclear Activities, United States. 2011 Available at: <https://www.oecd-nea.org/law/legislation/usa.pdf>. Accessed February 2014.
22. Pobanz, B. Private Communication. 25 October 2013
23. Reed, A. U.S. DOE's Response to the Fukushima Daiichi Reactor Accident: Answers and Data Products for Decision Makers. *Health Phys.* 102(5): 557-562; 2012.
24. Sandia National Laboratory. FRMAC Assessment Manual, Volume 1. Albuquerque, NM: Sandia National Laboratory; SNL Report, SAND; 2012.
25. Sandia National Laboratory. FRMAC Assessment Manual, Volume 3. Albuquerque, NM: Sandia National Laboratory; SNL Report, SAND; 2003.
26. Time Magazine Online. Time Photos [online]. Available at:
http://content.time.com/time/photogallery/0,29307,2058823_2276624,00.html.
Accessed 2 February 2014.
27. United States Geological Survey. EarthExplorer [online]. Available at:
<http://earthexplorer.usgs.gov>. Accessed 19 October 2013.

APPENDIX A

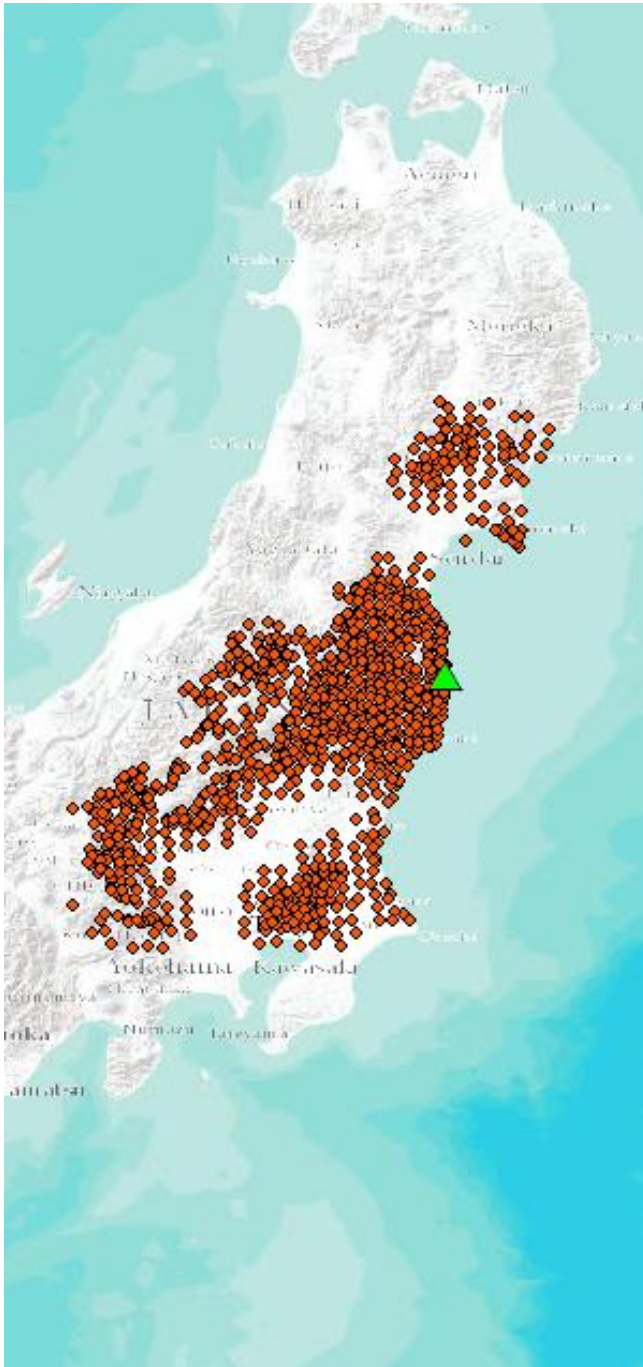


Fig. A- 1. 2nd Measurement *in situ* measurement locations.

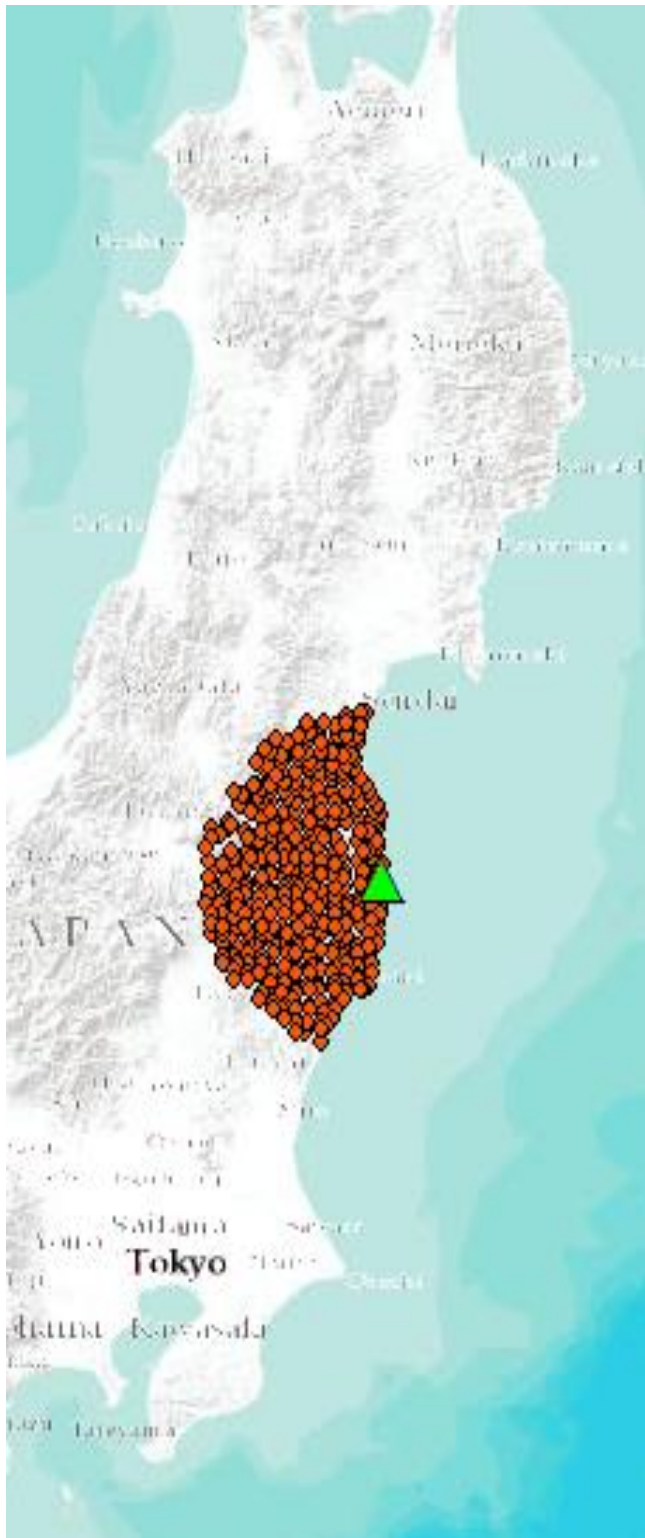


Fig. A- 2. 3rd Prophase *in situ* measurement locations.

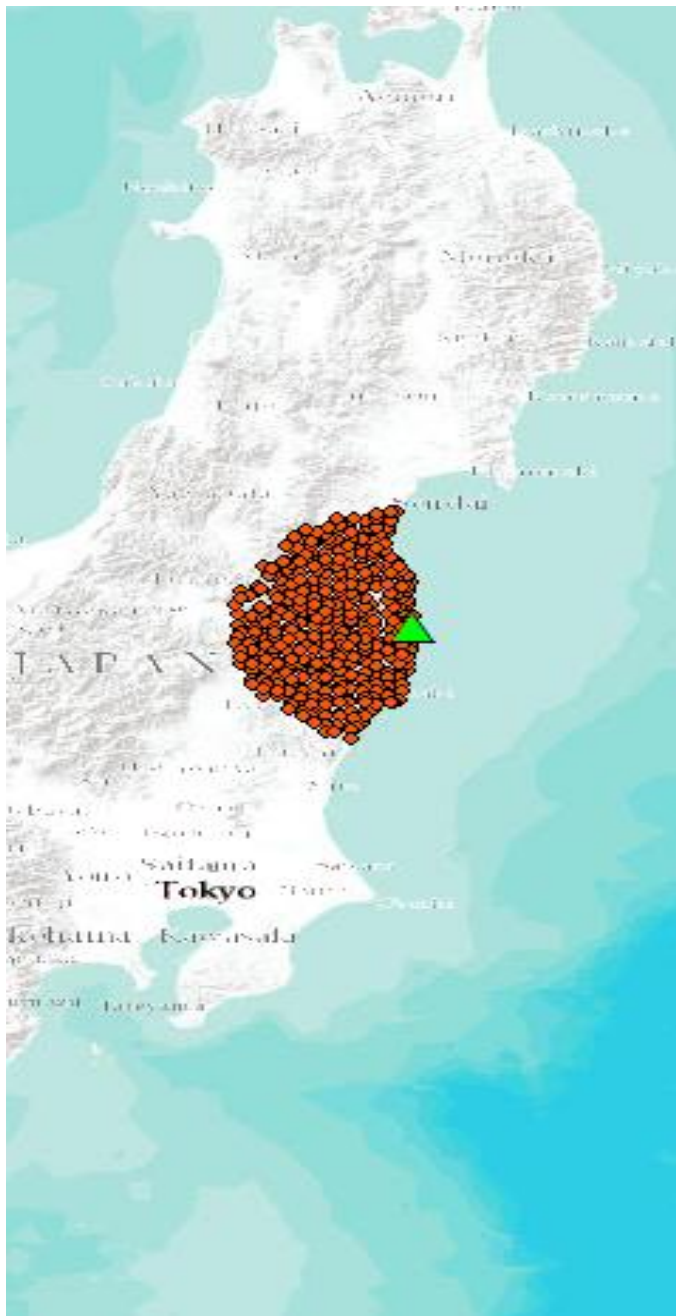


Fig. A- 3. 3rd Anaphase *in situ* measurement locations.

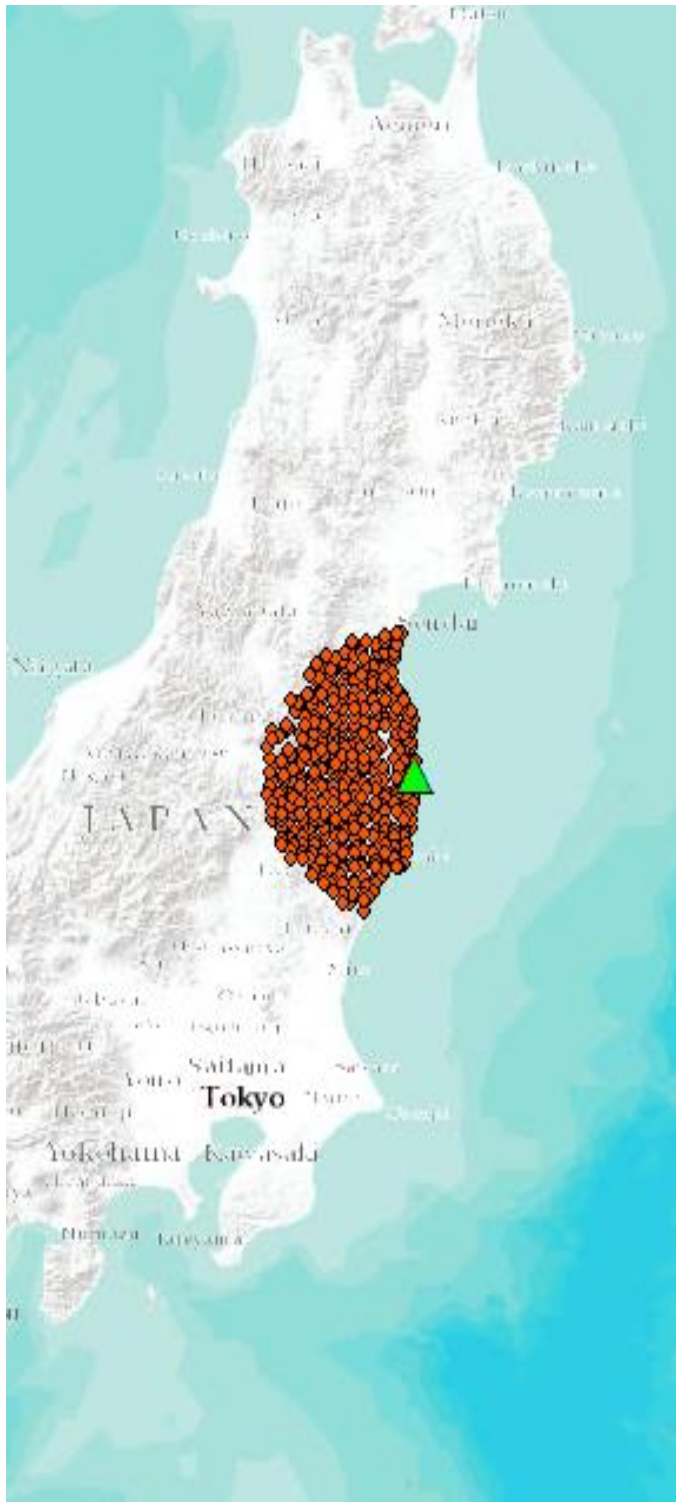


Fig. A- 4. 4th measurement *in situ* measurement locations.

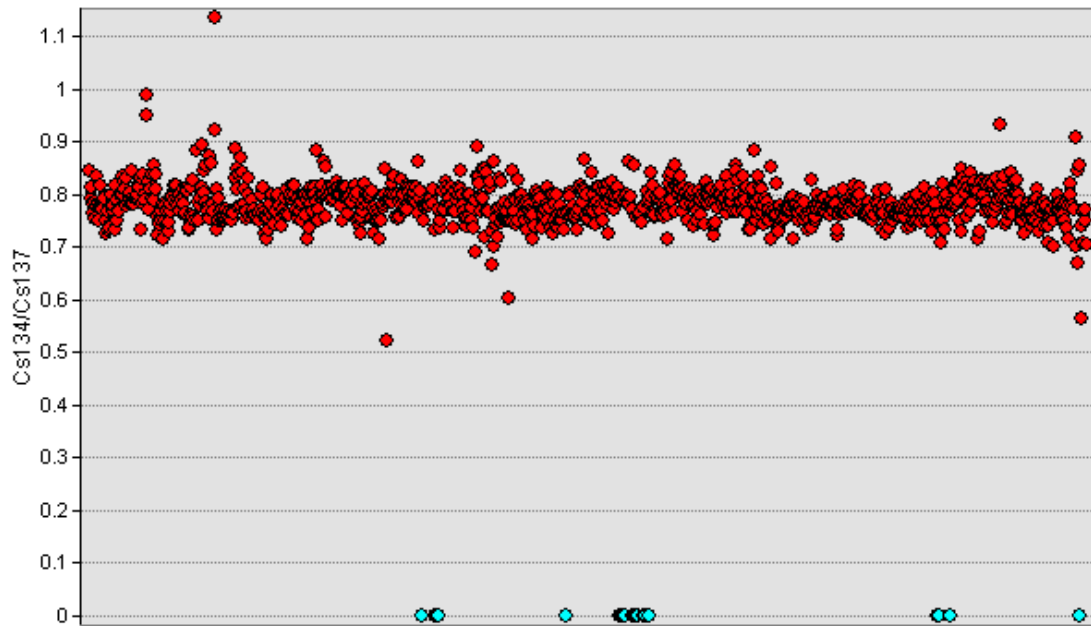


Fig. A- 5. Plot for $^{134}\text{Cs}/^{137}\text{Cs}$ concentration ratios from 2nd measurement.

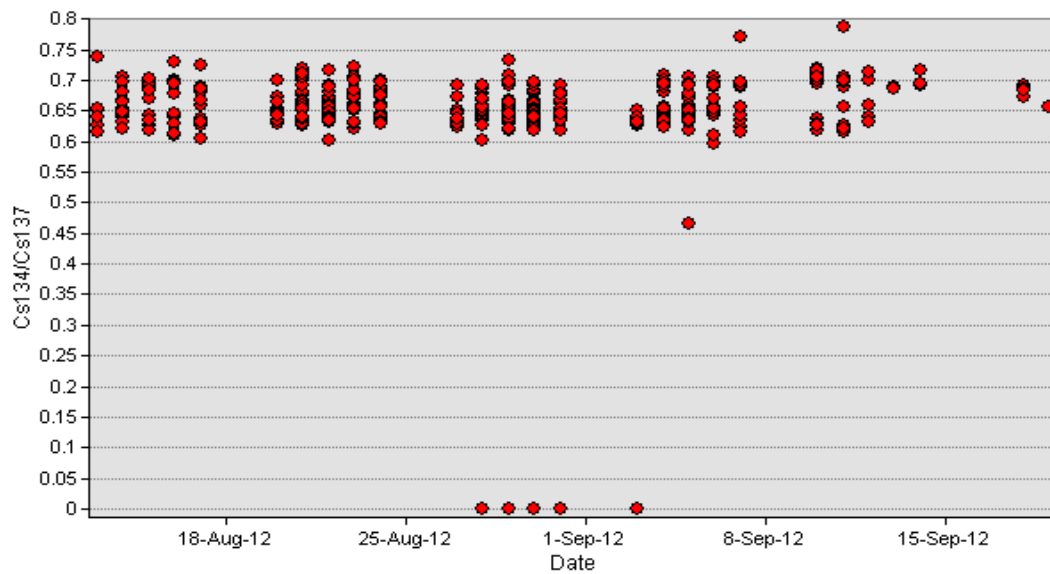


Fig. A- 6. Plot for $^{134}\text{Cs}/^{137}\text{Cs}$ concentration ratios from 3rd prophase measurement.

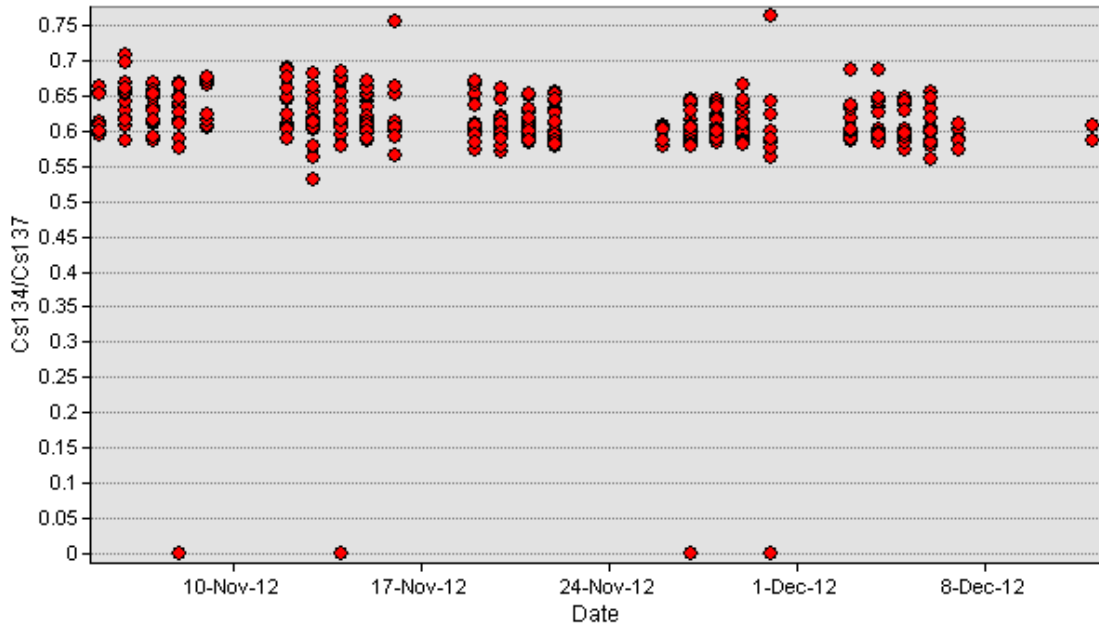


Fig. A- 7. Plot for $^{134}\text{Cs}/^{137}\text{Cs}$ concentration ratios from 3rd anaphase measurement.

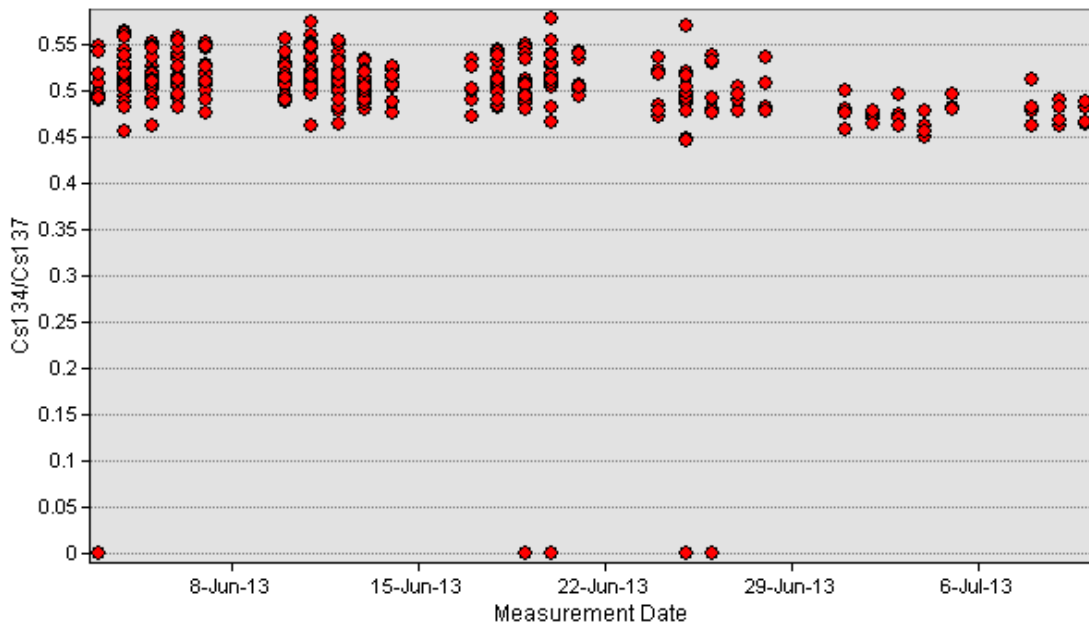


Fig. A- 8. Plot for $^{134}\text{Cs}/^{137}\text{Cs}$ concentration ratios from 4th measurement.